

## 6. SITE 778<sup>1</sup>

### Shipboard Scientific Party<sup>2</sup>

#### HOLE 778A

**Date occupied:** 22 February 1989  
**Date departed:** 24 February 1989  
**Time on hole:** 2 days, 12 hr, 55 min  
**Position:** 19°29.93'N, 146°39.94'E  
**Bottom felt (rig floor; m; drill-pipe measurement):** 3924.4  
**Distance between rig floor and sea level (m):** 10.7  
**Water depth (drill-pipe measurement from sea level; m):** 3913.7  
**Total depth (rig floor; m):** 4032.0  
**Penetration (m):** 107.6  
**Number of cores:** 13  
**Total length of cored section (m):** 107.6  
**Total core recovered (m):** 22.8  
**Core recovery (%):** 21  
**Oldest sediment cored:**  
Depth (mbsf): 107.6  
Nature: sheared phacoidal serpentinite  
Earliest age: (?)

**Hard rock:**  
Depth (mbsf): clasts  
Nature: serpentinitized tectonized harzburgite; dunite; metabasalt  
Measured velocity (km/s): 2.1 to 4

**Principal results:** Site 778 is situated about halfway up the southern flank of Conical Seamount, a 1500-m high, cone-shaped, serpentinite diapiric seamount located on the outer-arc high of the Mariana forearc basin, about 100 km west of the trench axis. Drilling established the presence of phacoidal sheared serpentinite beneath a serpentinite-rich clay-marl-breccia. Lithologic units are as follows:

1. Unit I (Subunit IA, 0–7.2 mbsf): The subunit contains lower/middle Pleistocene-Holocene serpentinite-rich sediment and serpentinite flows. The uppermost portion has two pebbles (one limestone and one serpentinite) overlying 15 cm of pale blue-gray serpentinite clay, then 15 cm of gray-green serpentinite clay, 10 cm of red-orange serpentinite clay, 1.5 m of pale blue-gray, silt-sized serpentinite and 3.57 m of a serpentinite-marl breccia.

2. Unit I (Subunit IB, 7.2–29.8 mbsf): The subunit is lower-middle Pleistocene to lower Pleistocene and contains a sandy marl and a collection of cobbles and pebbles, including serpentinite, vesicular volcanic rocks, and a foraminifer-bearing, serpentinite sandstone.

3. Unit II (29.8–107.6 mbsf): This entire unit is made up of phacoidal, sheared serpentinite containing clasts of serpentinitized tectonized harzburgite with subordinate metabasalts, metagabbros, serpentinitized dunite, and a variety of vein materials.

The serpentinite clays provide the strongest evidence that at least part of the seamount originated as serpentinite flows. The phacoidal sheared serpentinite may have originated as flows, as a mantle diapir, or both.

The primary petrology of the ultramafic rocks (% clinopyroxene predominantly as exsolution lamellae) indicates a depleted mantle source. The metabasalt clasts in Unit II have petrological and geochemical signatures of both mid-ocean ridge basalt and island-arc tholeiite types, and a few exhibit medium-grade metamorphism. One contains blue amphibole, perhaps indicating that this metamorphic grade characterizes the source region of the serpentinite. The material as a whole exhibits a variety of deformation textures that can be interpreted in terms of a combination of primary mantle tectonism, stresses related to intrusion and protrusion (flow emplacement) of the serpentinite diapir materials, and stresses resulting from post-protrusion remobilization.

Analyses of interstitial pore-water samples indicate a 10% decrease in chlorinity downhole (more than 107 m). Seep fluids are thought to have formed in part as a product of dehydration reactions within the subducting Pacific Plate. The decrease in chlorinity with depth in the hole is interpreted as a relative decrease in admixture of seawater with relatively chlorine-poor fluids entrained in the serpentine flow material.

#### BACKGROUND AND SCIENTIFIC OBJECTIVES

Site 778 is the first of a series of sites (778 through 780) on Conical Seamount, a roughly circular seamount having a basal diameter of about 20 km and a relief of 1500 m that lies on the outer-arc high of the Mariana forearc, at a distance of about 100 km from the trench axis (see "Introduction," this volume, and Fig. 1). The site was chosen to penetrate the flank of the seamount about 5.5 km due south of its summit. *Alvin* dives near this site suggested that the seamount in this area had been mantled by recent flows of unconsolidated serpentinite sediments and flows containing serpentinitized clasts of mafic and ultramafic rocks (Fryer et al., 1985). SeaMARC II side-scanning sonar imagery (Hussong and Fryer, 1985) further suggested that the site is located within a major serpentinite flow (delineated by an area of high sonic backscatter) that mantles much of the southern flank of the seamount (Fig. 2).

The specific objectives for drilling this flank site were to study the following aspects of forearc processes:

1. The internal stratigraphy and the extrusion and deformation history of a typical forearc serpentinite seamount;
2. The mode of emplacement of serpentinite flows;
3. The chemical effects of serpentinitization on the oceanic lithosphere and its sedimentary cover;
4. The nature, composition, and age of forearc lithosphere; and
5. The dewatering of subducted oceanic lithosphere at a nonaccretionary convergent plate margin.

The first objective was best achieved by a flank site, such as that chosen to penetrate the complete sequence of flows and to reach underlying sediments and basement. The depth of Site 778 is about 500 m above the background seafloor, and the normal sediment thickness in this area is estimated as about 250 m. Thus, drilling calculations were based on a 750-m hole that would penetrate the seamount and the underlying sediment, and perhaps also a short distance into basement if sediment thickness

<sup>1</sup> Fryer, P., Pearce, J. A., Stokking, L. B., et al., 1990. *Proc. ODP, Init. Repts.*, 125: College Station, TX (Ocean Drilling Program).

<sup>2</sup> Shipboard Scientific Party is as given in the list of participants preceding the contents.

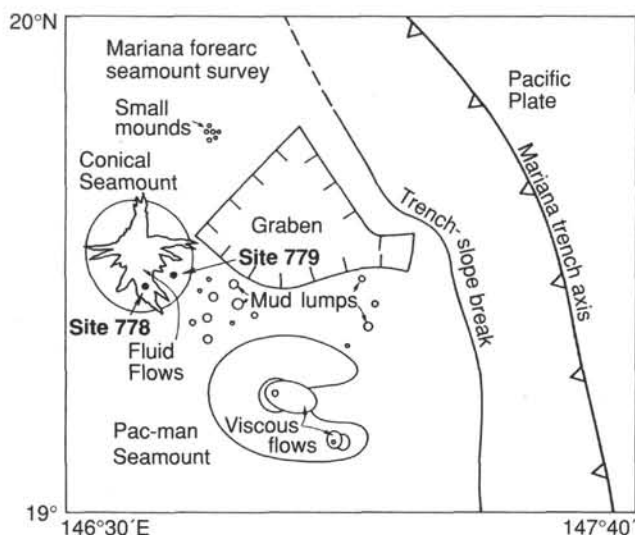


Figure 1. Geological sketch of Mariana forearc geology.

was low or the seamount had uplifted the surrounding seafloor. If successful, the hole would provide data about many unknown aspects of the construction of this serpentinite seamount, including thickness of flow and age of emplacement. The site location, about halfway down the flank, would also favor the second, sedimentary, objective by providing a typical (central) section through at least one serpentine flow within which sedimentary structures could be observed.

The third objective, the study of serpentinization, could be investigated using the mineralogy and composition both of the clasts, veins, and matrix within the serpentine flows, and of the sediments intercalated between and underlying these flows. The compositions of fluids entrained within the serpentine material and sediments should provide additional information about the chemical reactions involved and test whether, as in examples exposed on land, the fluids are of high pH and contain hydrogen and hydrocarbons. These compositions also could be used to investigate the relative roles of subducted water, primary mantle water, and surface seawater in the serpentinization process.

The nature of forearc lithosphere, the fourth objective, could be studied directly from any un-serpentinized ultramafic rocks and mafic clasts, and from the basement itself, should it be penetrated. Forearc basement is still poorly characterized. It is dependent on limited information from four previous drill sites (Leg 60), from dredging near Conical Seamount, and from the few on-land examples, such as those on Guam, Saipan, and the Bonin Islands; we still know little about the composition of forearc basement in submarine, sedimented regions. Although the vast majority of basement volcanic samples have proved to exhibit boninitic to depleted island-arc tholeiitic compositions, mid-ocean ridge basalts may also contribute to forearc basements, especially if trapped older crust is present. A further possibility is that clasts may include samples of Pacific oceanic crust that might have been accreted onto the forearc mantle wedge from the Benioff Zone and incorporated into serpentinite diapirs at depth. Pacific crustal fragments should have a composition quite distinct from the forearc crust, but if *in-situ* basement could be penetrated at this site, this distinction should be easier to make. In addition, the study of textures of clasts within the serpentinite should aid in determining both the stress history of the forearc during serpentinization and the emplacement mechanisms of the diapiric body. Information about all these rocks should also

aid our understanding of the many ophiolite complexes that have been postulated to have occupied a forearc setting.

Finally, the objective of studying the hydration of the crust and upper mantle of the forearc wedge could be accomplished by drilling into the serpentinite. The hydration of the forearc wedge has been clearly facilitated by the escape of fluids from the subducting Pacific plate, and thermal modeling suggests that large regions beneath the forearc lie within the chlorite, greenschist, and blueschist stability fields (Fryer and Fryer, 1987). The mantle and lower crust of the forearc wedge can thus readily accommodate large volumes of fluids through metamorphic processes. The exact nature of fluid transport is poorly understood, although it can be assumed that, under appropriate tectonic conditions, generation and emplacement of serpentinite diapirs is a major factor in any non-accretionary forearc. Analyses of hydrous phases could provide evidence for the magnitude of fluid fluxes within the mantle wedge and for the temperatures and compositions of these fluids, while studies of metamorphic assemblages in the clasts should further constrain the pressure/temperature history of metamorphism within the forearc.

## OPERATIONS

### Guam Port Call

Leg 125 officially began when the first line was passed at 2000 hr UTC (Universal Time Coordinated), 15 February 1989, and the *JOIDES Resolution* (SEDCO/BP 471) arrived at Apra Harbor, Guam. The normal operations of crew changes, fueling, and on/off loading of all freight were performed without problems. The ship sailed on schedule, leaving Apra Harbor, Guam at 0200UTC, 20 February.

### Guam to Site 778 (MAR-3B)

The 35-hr transit to the Mariana sites was made in calm weather and seas. The *JOIDES Resolution* did not arrive in the vicinity of the Mariana sites during a global positioning system (GPS) window. The location of proposed Site MAR-3A was critical, but could not be determined without GPS. Therefore, proposed Site MAR-3B was drilled first.

### Site 778 (Hole 778A)

Site 778 is located on the southern flank of Conical Seamount. Site 778 was established by dropping a recoverable beacon at 2030UTC, 21 February after 5 hr of surveying.

Based on information from *Alvin* photographs and video tapes of Conical Seamount, the hole was spudded with the rotary coring system (RCB) instead of the advanced piston corer/extended-core barrel (APC/XCB). A standard RCB bottom-hole assembly (BHA) with mechanical bit release (MBR) and bit was assembled and run. The mud line was established at 3913.7 m below sea level (bsl) by a punch core at 1445UTC 22 February. The precision depth recorder showed the mud line at 3754.8 m below sea level (bsl); it took 6 hr to find the bottom.

The hole was unstable from the beginning and soon caused problems. After reaching Core 125-778A-4R at 3943.3 mbsl, the hole required cleaning upon each connection. During retrieval of Core 125-778A-13R, the hole caved in and the drillpipe stuck. The drill string was worked with 20,000-lb overpulls before the BHA was freed. During repeated attempts to clean the hole, the drill string stuck again, whereupon the hole was abandoned.

The RCB was used for the entire hole, where we recovered 22.8 m in 13 deployments for a recovery rate of 21% (Table 1). Hole 778A and Site 778 were officially abandoned at 0925UTC, 24 February, when the drill string was pulled clear of the seafloor.

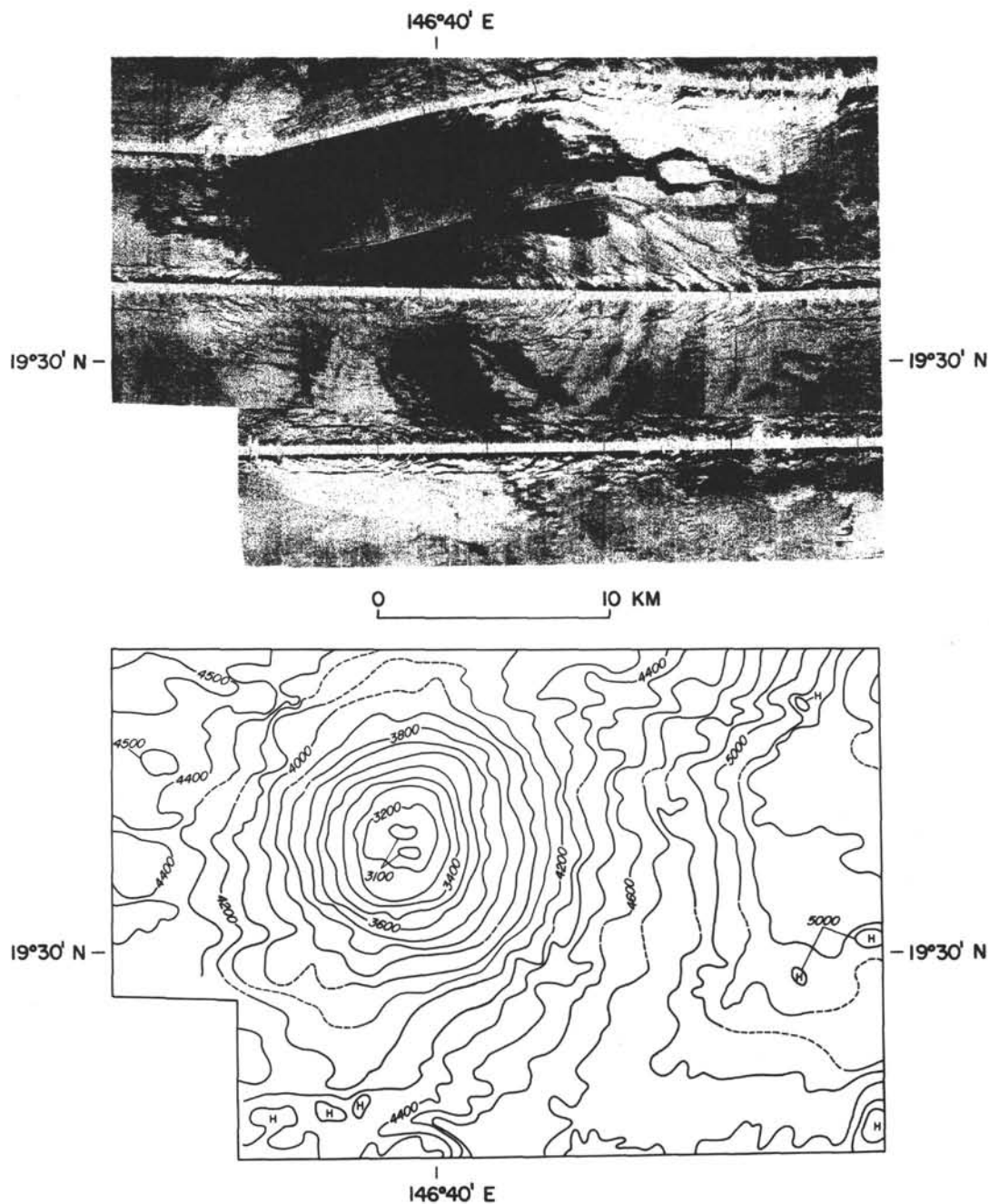


Figure 2. A. SeaMARC II side-scanning image of Conical Seamount. B. Bathymetric map of Conical Seamount showing the locations of Leg 125 drill sites.

## LITHOSTRATIGRAPHY

### Lithologic Summary

The stratigraphic section recovered at Site 778 is divided into two lithologic units (I and II) based upon composition, color, and degree of lithification. Lithologic Unit I consists of clay, marl, silt-sized serpentine, serpentine breccia, and pebbles of various lithologies. The lower unit, Unit II, is composed of serpentine breccia with phacoidal and sheared textures and some convolute structures. Intervals of serpentinized ultramafic cobbles and pebbles are also present in lithologic Unit II (Table 2).

### Coring Disturbance

A significant portion of the stratigraphic section at this site was not recovered. Groups of pebbles, lacking an associated matrix, occur at tops and bases of longer cores (midsections contain sediment or serpentine), or as the only material recovered in shorter cores. This relationship argues for removal of fine-grained sediment and serpentine by washing during coring. The uppermost stratigraphic successions recovered from Hole 778A certainly demonstrate coring disturbances. For instance, the intercalated, pale-blue, silt-sized serpentine in Section 125-778A-1R-1 between 12 and 13 cm appears to have been emplaced artificially; and a serpentine

**Table 1. Coring summary for Hole 778A.**

Core no.	Date (Feb. 1989)	Time (UTC)	Depth (mbsf)	Length cored (m)	Length recovered (m)	Recovery (%)
1R	22	1540	0.0–6.7	6.7	6.70	100.0
2R	22	1700	6.7–16.2	9.5	1.03	10.8
3R	22	1910	16.2–20.2	4.0	0.18	4.5
4R	22	2200	20.2–29.7	9.5	0.24	2.5
5R	23	0235	29.7–39.2	9.5	0.43	4.5
6R	23	0550	39.2–48.7	9.5	1.70	17.9
7R	23	0810	48.7–58.2	9.5	2.54	26.7
8R	23	1110	58.2–68.2	10.0	1.66	16.6
9R	23	1600	68.2–77.8	9.6	2.16	22.5
10R	23	2012	77.8–82.3	4.5	0.22	4.9
11R	23	2350	82.3–89.8	7.5	1.75	23.3
12R	24	0305	89.8–98.3	8.5	2.40	28.2
13R	24	0700	98.3–107.6	9.3	1.79	19.2
Coring totals				107.6	22.80	21.2

breccia with its sandy silt matrix has been disrupted, resulting in the soupy appearance of the core in Section 125-778A-1R-2 from 37 to 130 cm.

### Unit I

Sections 125-778A-1R-1, 0 cm, to 125-778A-5R-1, 10 cm; depth, 0–29.8 mbsf. Age: Holocene(?) to lower Pleistocene(?).

Only Unit I contains sediment with detrital and biogenic components at this site. The serpentinite intervals lack biogenic and detrital components but are underlain by sediment of late Pleistocene age, indicating a maximum age of late Pleistocene for the serpentinite flow(s) (see "Biostratigraphy" and "Paleomagnetism" sections, this chapter).

#### Subunit IA

Sections 125-778A-1R-1, 0 cm to 125-778A-2R-1, 50 cm; depth, 0–7.2 mbsf. Age: Holocene(?) to lower/middle Pleistocene.

This subunit extends from the sediment/water interface to a total depth of 7.2 mbsf and primarily consists of serpentinite clay, and silt-sized serpentinite, with sand- to pebble-sized

clasts of serpentinite. The uppermost lithology in the first core has two pebbles (recrystallized limestone and a serpentinitized ultramafic rock) atop 15 cm of gray-green (2.5Y 6/2) serpentinite clay that has been disturbed by drilling. In addition, the serpentinite clay contains opaque minerals (10%), epidote (5%), zoisite (5%), aragonite (10%), nanofossils (5%), and trace amounts of radiolarians and silicoflagellates. Beneath this serpentinite clay is a 10-cm-thick sequence of red-orange (5YR 6/8) serpentinite clay that has a sharp lower contact. This 10-cm-thick layer of clay has crystalline clay aggregates and lacks biogenic components. The color, composition, and nongradational lower contact of this clay layer may indicate a cool hydrothermal origin or post-depositional alteration by migration of fluids from the underlying serpentinite flow. This red-orange clay overlies a 1.5-m layer of pale blue-gray (5B 6/2) silt-sized serpentinite that is composed of serpentinite (80%), opaque minerals (10%), zoisite (5%), epidote (5%), with trace amounts of chlorite, and thulite. This 1.5-m-thick serpentinite layer is interpreted as a serpentinite flow that extruded onto the seafloor under cool hydrothermal conditions because (1) it lacks pelagic or detrital components, (2) the color is atypical of pelagic sediments, and (3) biological and sedimentological structures are absent.

Beneath this is a 0.9-m interval of breccia that has been strongly disturbed by drilling. It contains a matrix of sandy clay, perhaps equivalent in lithology to the underlying 4.0-m-thick layer of serpentinite breccia with a matrix of sandy silt-sized serpentinite. The lithologies of clasts within the breccia are described in the "Igneous and Metamorphic Petrology" section (this chapter). In the breccia, the sandy silt-sized serpentinite matrix is light reddish brown (2.5Y 6/4) and composed of serpentinite (60%), opaque minerals (15%), aragonite (15%), and epidote (10%). Mixed into the 4.0-m-thick layer, yielding a mottled appearance, is light gray (7.5YR 7/0) and light olive (5Y 5/2) serpentinite-chlorite-rich marl (chlorite, 25%; serpentinite, 20%; opaque minerals, 15%; micrite, 15%; nanofossils, 10%; aragonite, 10%; clay, 5%; trace amounts of epidote and zoisite) of Pleistocene age. The depositional mechanisms of this layer are not clear. Its similarity to the overlying blue layer (in all but color) may indicate that it is also a flow, in which case the mottling represents entrained

**Table 2. Lithologic units recovered at Leg 125 Site 778.**

Lithologic unit	Cores	Depth (mbsf)	Dominant lithology	Stratigraphic age
IA	778A-1R-1, 0 cm to 778A-2R-1, 50 cm	0.0 to 7.2	Clay; marl; clayey silt-sized serpentinite; serpentinite breccia with a matrix of sand- and silt-sized serpentinite	Holocene(?) to lower/middle Pleistocene
IB	778A-2R-1, 50 cm to 778A-5R-1, 10 cm	7.2 to 29.8	Sandy marl; volcanoclastic(?) siltstone; foraminifer-bearing serpentinite sandstone; various igneous lithologies (see "Igneous and Metamorphic Petrology," this chapter)	lower/middle Pleistocene to lower Pleistocene(?)
II	778A-5R-1, 10 cm to 778A-13R-CC	29.8 to 107.6	Phacoidal sheared serpentinite; serpentinite breccia with convolute structure; pebbles of various lithologies (see "Igneous and Metamorphic Petrology," this chapter)	(?)

Table 3. X-ray diffraction analysis of samples, Site 778.

Core, sample, interval (cm)	Method of preparation	Identified Minerals													
		An	Cr	T	B	A	G	C	E	Z	Ga	St	Fo	Fa	
125-778A-1R-1, 20	pip		x	x	x	x	x	?	?	x					
1R-1, 20	pow		x	x	x		x							x	
1R-1, 100	pip		x	x			x		x	x					
1R-1, 100	pip		x	x			x	x	?			x			
1R-1, 100	pow		x	x	x		x	x			x				
1R-4, 50	pip		x	x	x		x	x					x		
1R-4, 50	pow		x	x	x										
1R-4, 60	pip		x	x	x		x				x		x		
1R-4, 60	pow		x	x	x		x	x				x	x		
1R-4, 125	pip		x	x	x		x		?						
1R-4, 125	pow		x	x	x		x								
1R-4, 125	pow		x	x	x			x	x	?					

Note: pip = oriented pipette sample; pow = powder sample; An = antigorite; Fo = forsterite; Cr = chrysotile; Fa = fayalite; T = talc; B = brucite; A = aragonite; G = goethite; C = chlorite; E = enstatite; Z = zoisite; Ga = garnierite; St = stevensite.

pelagic sediment. On the other hand, the mottling may have resulted from coring disturbance. The reddish brown color suggests sufficient seafloor exposure to allow oxidation.

Aragonite in these water depths is unusual - the aragonite compensation depth is approximately at a water depth of 600 m at this site. The delicate, acicular habit of the aragonite crystals (up to 3 mm in length, 0.5 mm in width) in the clay and serpentine imply post-emplacement authigenic growth.

#### Subunit IB

Sections 125-778A-2R-1, 50 cm, to 125-778A-5R-1, 10 cm; depth, 7.2–29.8 mbsf. Age: lower/middle Pleistocene to lower Pleistocene(?).

This subunit is defined on the basis of an interval of poor recovery, resulting in a collection of cobbles and pebbles, possibly representing drilling breccia. In Section 125-778A-3R-CC (the only section recovered for that core), a sandy marl (clay, 30%; micrite, 25%; nannofossils, 10%; opaque minerals, 10%; zoisite, 10%; epidote, 5%; serpentine, 5%; chlorite, 5%) coated a serpentized ultramafic pebble. A thin section of a pebble (Sample 125-778A-4R-1, 5–6 cm) revealed a clay matrix containing trace amounts of poorly preserved radiolarians and Neogene planktonic foraminifers among coarser grains of vesicular volcanics and crystals of olivine. The absence of pyroxene and feldspar crystals suggests that the source rock may be dunite. The lowest pebble in this section is a foraminifer-bearing serpentine sandstone of Pleistocene age composed of serpentine (65%), opaque minerals (12%), epidote (10%), chlorite (5%), aragonite (5%), foraminifers (3%), and a trace amount of nannofossils. Biostratigraphic criteria suggest that the vertical succession of sedimentary pebble occurrences may be stratigraphically correct. Igneous lithologies of additional pebbles interspersed in this subunit are described in the "Igneous and Metamorphic Petrology" section (this chapter).

#### Unit II

Sections 125-778A-5R-1, 10 cm, to 125-778A-13R-CC; depth, 29.8–107.6 mbsf.

This unit is primarily composed of phacoidal sheared serpentine and intervals of serpentine breccia having a convolute structure. A description and discussion of the breccia clast lithologies are given in the "Igneous and Metamorphic Petrology" section (this chapter). The matrix of the breccia is composed of serpentine (50%–80%), opaque minerals (20%–5%), thulite (25%–0%), epidote (20%–0%), chlorite (15%–

0%), zoisite (10%–0%), talc (5%–0%), olivine (5%–0%), and trace to 0% of albite. Convolute structures appear in Sections 125-778A-6R-1 at 85 to 150 cm, 125-778A-8R-1 at 60 to 132 cm, 125-778A-9R at 75 to 150 cm, all of Core 125-778-12R, and Section 125-778A-13-1 at 25 to 140 cm. These deformation structures may have been produced by purely tectonic or purely gravitational flow processes (for further discussion see "Structural Studies" section, this chapter).

#### X-Ray Diffraction Analysis

Mineral identification of five samples from Site 778 was conducted using X-ray diffraction (XRD) on both powder (pow) and oriented pipette (pip) samples. Powder samples were dried, ground manually in an agate mortar, and packed in a sample holder. Pipette samples were prepared from the <4-mm fraction, which was separated by sedimentation in a 20-mL beaker. Preliminary mineral identification is listed in Table 3.

All samples contain both serpentine groups, and it seems that the 2- as well as the 20-Modification of chrysotile is present. Almost all samples contain brucite. Olivine, epidote-zoisite, and aragonite are present. Confirmation of the occurrence of chlorite, goethite, stevensite (a mixed-layered structure of talc/saponite), and garnierite must be left to future shore-based investigations.

#### BIOSTRATIGRAPHY

Evidence from calcareous nannofossils and planktonic foraminifers indicates that the sedimentary interval overlying the serpentinite ranges in age from early/middle Pleistocene to early Pleistocene. Microfossils were found only in samples from Cores 125-778A-2R and 125-778A-4R. No diatoms were recovered from any of the cores.

#### Calcareous Nannofossils

A well-preserved, but rare, Quaternary nannofossil assemblage is present in Section 125-778A-2R-1. This core is early/middle Pleistocene (Zone CN14a; Okada and Bukry, 1980) in age, based on the occurrence of *Gephyrocapsa oceanica* and *Pseudemiliania lacunosa*, together with the lack of *Emiliania huxleyi*.

Moderately preserved Quaternary nannofossils are common in Sample 125-778A-4R-CC. This core has been dated early Pleistocene (Subzone CN14a; Okada and Bukry, 1980) by the co-occurrence of *Gephyrocapsa caribbeanica*, *G. oceanica*, and *Calcidiscus macintyreii*. Its absolute age is approximately 1.45 Ma.

## Foraminifers

Late Pliocene-Pleistocene foraminiferal assemblages were recovered from Section 125-778A-2R-1, and Samples 125-778A-4R-1, 23–25 cm, and 125-778A-4R-CC. All contain relatively rare, poorly preserved wide-ranging taxa, dominated by *Globigerinoides immaturus* and *G. quadrilobatus* and less common *Orbulina universa*, *Globigerinella aequilateralis*, *Sphaeroidinella dehiscens*, *Globorotalia (M.) menardii*, *G. tosaensis*, and *G. truncatulinoides*.

A late Pliocene to Pleistocene age (Zone N21-N22) was obtained from planktonic assemblages in Section 125-778A-2R-1 and Sample 125-778A-4R-CC. The presence of *Globorotalia truncatulinoides* in Section 125-778A-2R-1 and Sample 125-778A-4R-CC effectively confines this section (and the sections above) to the Pleistocene (Zone N22), owing to the restriction of *G. truncatulinoides* to Zone N22, as shown by Kennett and Srinivisan (1983). *G. tosaensis* and *G. truncatulinoides* are common components of warm subtropical to tropical water assemblages.

## IGNEOUS AND METAMORPHIC PETROLOGY

The following section describes ultramafic, mafic, and other types of clasts that occur both as isolated fragments and as inclusions in a matrix of sheared and deformed, fine-grained serpentine. The characteristics of this matrix are described in the "Structural Studies" section (this chapter). We interpret these clasts as representative of the basement lithologies incorporated during the ascent of the serpentinite. Several different types of clast are present. The majority (80% by volume) are serpentized ultramafic rocks, mostly of tectonized harzburgite and subordinate dunite protoliths. The remainder are predominantly metabasalts (15%), together with rare metagabbros, talc, and vein minerals. Clast sizes range from about 15 cm to less than 1 mm.

### Ultramafic Clasts

#### *Serpentinized Tectonized Harzburgites*

These clasts range in color from a deep blackish-green to a light dun. In many samples, veining by serpentine and carbonate leads to small-scale color variations. Although most are massive, some are foliated by the alignment of bastitic orthopyroxene. Chrome spinels are sometimes dumbbell-shaped and occasionally form stringers defining a lineation.

The primary mineralogy has been pervasively altered to serpentine; however, relict orthopyroxene, olivine, clinopyroxene, and apparently fresh chrome spinel are preserved. Serpentinized olivine (about 80–95 modal %) forms a massive mesh-textured fabric having no obvious crystal outlines. Orthopyroxene (bastite; 5–20 modal %; <10 mm in maximum dimension) is typically kink-banded and sometimes elongate. Exsolution lamellae of clinopyroxene along the (100) plane of host orthopyroxene usually have undulose extinction. Relict clinopyroxene (<1 mm in size) is also present in the margins of some orthopyroxene crystals. Preliminary petrographic observations indicate that both olivine and orthopyroxene are highly magnesian. Chrome spinel (<1 mm in size) occurs as disseminated and isolated anhedral grains.

Serpentine dominates the secondary mineralogy and appears mostly to be antigorite or lizardite. Vein serpentine has a fibrous habit, orientated orthogonal to vein walls and is probably chrysotile. Vein carbonate is microcrystalline, whitish-green, and may include subordinate brucite, epidote, and manganese-rich zoisite (thulite). Veins are 0.1 to 1 mm wide and up to 2 cm long.

### *Serpentinized Dunites*

The color of these rocks varies from black to dun, with some local mottling where veined. The primary mineralogy consists of 95% serpentized olivine, with about 5% orthopyroxene and up to 1% chrome spinel. A mesh texture characterizes these clasts. Bastite pseudomorphs of orthopyroxene are apparently undeformed and are up to 5 mm in size. Spinel is euhedral, <1 mm in size, and forms local bands (up to 10 mm wide) of disseminated grains.

### *Talc-Serpentine*

Two clasts of this type were recovered. The clasts are light greenish-white, have a soapy feel, and are very soft (Mohs' scale hardness of 2). The mineralogy is essentially talc and serpentine, with trace amounts of chrome spinel.

## Mafic Clasts

### *Metabasalt*

These clast types are generally dark grayish-green to light gray, ranging in size from a few centimeters (most common) to 10 cm (rare). Most have a subrounded shape, a margin containing patches of shiny black serpentine, and generally a massive internal structure. A minority of samples are cataclastic and contain 1- to 5-mm-wide shear zones; others are brecciated with individual (now recemented) grains 1 to 6 mm in size.

Two variably metamorphosed fine- to medium-grained metabasalts have been identified: plagioclase-clinopyroxene plus orthopyroxene pyritic in a glassy groundmass; and orthopyroxene-olivine-chrome spinel-pyritic in a glassy groundmass. Several clasts have quench-textures (skeletal and swallow-tailed plagioclase; spinifex pyroxene), but most have a felted texture formed from now-altered plagioclase laths in a more mafic, altered, fine-grained groundmass. Oxide minerals, mainly magnetite, are present in small abundances in some samples.

Many of the metavolcanic clasts are veined by carbonate, chlorite, and epidote. Vein orientations appear to be random. Amygdules composed mostly of chlorite (<0.5 to 1.0 mm) commonly form less than 1% of the rocks.

### *Metagabbro*

Only one example of this type of clast was recovered. In hand specimen the rock is medium- to fine-grained with about 40% plagioclase and 60% mafic phases forming an isotropic texture.

## Other Clast Types

This category includes rare, angular fragments of vein-type carbonate, quartz, and amphibolite (<30 cm in diameter). Some of these clasts are partially jacketed with sheared serpentine clay, but most form separate fragments, together with the metabasalt clasts. Both coarsely polycrystalline (0.5–5 mm) and more fine-grained materials are present. A brownish-orange material, apparently a chert fragment, forms an angular (about 2 cm) fragment in one core. One small clast contains fragments of both coarse- and fine-grained amphibolite (possibly from a basic igneous protolith) in a fine-grained, schistose and chloritic matrix. The amphiboles are pale green hornblende rimmed with blue amphibole, possibly crossite or glaucophane. The original nature of this clast is unclear; it may have been a sedimentary or tectonic breccia.

## IGNEOUS AND METAMORPHIC GEOCHEMISTRY

Shipboard geochemical analyses of clasts entrained within serpentine at Site 778 were performed for 10 samples of

**Table 4. Major-element data for serpentinized, ultramafic rocks from Hole 778A.**

Core: Interval (cm):	2R-1 53-56	2R-1 89-92	3R- CC 1-7	7R-2 73-78	7R- CC 7-13	8R-1 36-44	12R-2 43-45	12R-2 73-75	13R-1 15-17	13R-2 8-11
SiO <sub>2</sub>	38.17	35.69	40.93	34.14	37.46	34.61	41.52	39.29	37.10	49.99
TiO <sub>2</sub>	0.00	0.00	0.00	0.00	0.00	0.00	0.00	0.00	0.00	0.00
Al <sub>2</sub> O <sub>3</sub>	0.74	0.00	1.09	0.85	0.76	0.68	0.71	1.01	0.47	4.54
Fe <sub>2</sub> O <sub>3</sub>	6.73	6.77	7.21	8.66	7.86	8.00	8.95	7.64	7.88	6.92
MnO	0.10	0.10	0.10	0.14	0.13	0.16	0.08	0.06	0.11	0.18
MgO	36.59	35.88	36.85	39.32	39.15	39.21	39.61	37.04	39.38	22.65
CaO	0.07	3.52	0.74	0.02	0.03	0.08	0.06	0.07	0.79	8.45
Na <sub>2</sub> O	0.09	0.09	0.00	0.09	0.00	0.00	0.00	0.00	0.00	0.51
K <sub>2</sub> O	0.01	0.00	0.01	0.01	0.05	0.00	0.00	0.00	0.00	0.02
P <sub>2</sub> O <sub>5</sub>	0.00	0.01	0.00	0.00	0.00	0.00	0.00	0.00	0.00	0.00
LOI	15.06	15.55	11.49	14.76	13.66	16.06	6.01	11.99	13.49	5.53
NiO	0.29	0.39	0.28	0.39	0.36	0.33	0.36	0.37	0.29	0.07
Cr <sub>2</sub> O <sub>3</sub>	0.36	0.07	0.37	0.41	0.33	0.37	0.42	0.53	0.27	0.12
Total	98.20	98.08	99.08	98.79	99.79	99.50	97.70	98.00	99.79	98.99

Data (in wt% oxides) are for whole-rock analysis by CXRF. LOI is loss on ignition between 150° and 1030°C.

**Table 5. Trace-element data for serpentinized, ultramafic rocks from Hole 778A.**

Core: Interval (cm):	2R-1 53-56	2R-1 89-92	3R- CC 1-7	7R-2 73-78	7R- CC 7-13	8R-1 36-44	12R-2 43-45	12R-2 73-75	13R-1 15-17	13R-2 8-11
Nb	tr	tr	tr	tr	tr	tr	tr	tr	tr	tr
Zr	1	2	0	1	1	1	0	1	1	2
Y	0	nd	1	nd	nd	nd	1	nd	0	2
Sr	9	595	5	2	3	8	9	12	3	31
Rb	0	nd	1	nd	1	1	nd	0	0	nd
Zn	52	28	36	39	42	64	42	40	37	38
Cu	3	3	11	2	2	4	8	2	14	9
Ni	2281	3039	2173	3034	2818	2638	2813	2905	2297	571
Cr	2496	501	2523	2786	2261	2510	2866	3603	1875	837
V	46	22	40	38	41	48	48	62	34	75
Ti	0	0	0	0	0	0	0	0	0	0
Ce	tr	tr	nd	tr	nd	nd	tr	nd	12	tr
Ba	tr	nd	tr	nd	nd	10	nd	nd	nd	tr

Data (in ppm) are for whole-rock analysis by XRF; nd = not detected, tr = below detection limits (<2 ppm for Nb; <10 ppm for Ba and Ce).

**Table 6. Major-element data for mafic rocks from Hole 778.**

Core: Interval (cm):	5R-1 7-10	11R-1 0-3	9R-CC 9-12	11R-1 5-8	13R-1 5-8	13R-1 12-14	13R-CC 4-6
SiO <sub>2</sub>	56.03	45.19	46.44	46.07	42.57	40.01	40.78
TiO <sub>2</sub>	0.29	2.32	0.91	1.10	1.12	1.09	1.33
Al <sub>2</sub> O <sub>3</sub>	14.38	6.39	15.52	14.88	12.48	11.98	9.27
Fe <sub>2</sub> O <sub>3</sub>	8.20	18.21	8.44	12.84	11.97	10.60	10.00
MnO	0.16	0.25	0.17	0.17	0.25	0.23	0.22
MgO	7.57	11.73	7.66	2.52	6.73	16.94	21.81
CaO	3.01	9.27	12.29	9.24	17.38	10.10	6.19
Na <sub>2</sub> O	5.15	3.49	0.73	5.08	1.46	0.18	0.87
K <sub>2</sub> O	0.16	0.02	3.04	0.79	0.29	0.76	0.01
P <sub>2</sub> O <sub>5</sub>	0.03	0.23	0.14	0.04	0.07	0.08	0.10
<sup>a</sup> LOI	2.91	1.74	3.78	3.95	4.45	7.30	7.94
TOTAL	97.90	98.93	99.13	96.72	98.80	99.30	98.54

<sup>a</sup>Between 150° and 1030°C. Data (in wt% oxides) are for whole-rock analysis by XRF.

serpentinized, tectonized harzburgite and for seven samples of metabasalt. Preparation and analytical techniques are given in the "Explanatory Notes" (this volume). These data are given in Tables 4 through 7. Rock descriptions are presented in the "Igneous and Metamorphic Petrology" section (this chapter).

### Ultramafic Rocks

The original (pre-serpentinization) composition of these samples, based on modal estimates from thin-section descriptions, is approximately 70% to 95% olivine, 5% to 30%

**Table 7. Trace-element data for mafic rocks from Hole 778.**

Core: Interval (cm):	5R-1 7-10	11R-1 0-3	9R-CC 9-12	11R-1 5-8	13R-1 5-8	13R-1 12-14	13R-CC 4-6
Nb	tr	tr	tr	tr	tr	5	tr
Zr	31	150	50	60	64	57	78
Y	9	62	21	22	28	28	28
Sr	51	41	95	62	95	82	44
Rb	3	nd	57	16	6	17	nd
Zn	56	93	71	100	92	95	74
Cu	299	57	35	206	75	51	49
Ni	54	563	44	47	42	41	28
Cr	85	109	117	68	151	170	43
V	215	494	239	357	317	242	281
Ti	1739	13915	5458	6598	6718	6538	7977
Ce	tr	11	nd	nd	16	10	tr
Ba	tr	25	54	46	58	33	14

nd = not detected; tr = below detection levels (<5 ppm for Nb; <10 ppm for Ba and Ce). Data (in ppm) are for whole-rock analysis by XRF.

orthopyroxene, and <1% clinopyroxene and spinel. The degree of serpentinization ranges from 50% to 95%.

### Major Elements

Overall, the ultramafic rocks analyzed are quite homogeneous in both major and trace element chemistry.

Loss on ignition (LOI) is high in these samples (Table 4), ranging from 5.53 to 16.06 wt%. These values clearly result from serpentinization, although there is no obvious correlation between LOI and observed percentage of serpentiniza-

tion. LOI only includes volatile loss between 110° and 1030° and thus represents H<sub>2</sub>O<sup>+</sup> and CO<sub>2</sub>. The upper range of LOI values is similar to that reported from DSDP Leg 82 for serpentinized peridotites recovered from the Middle Atlantic Ridge (12.86–16.07 wt%, Michael and Bonatti, 1985); however, the lower values (5.53 and 6.01) are significantly smaller. Total percentages of major elements are typically 98 to 100 wt% (including Cr<sub>2</sub>O<sub>3</sub> and NiO); MgO ranges from 27.30 to 39.61 wt% and SiO<sub>2</sub> ranges from 34.14 to 41.52 wt%. Total iron, calculated as Fe<sub>2</sub>O<sub>3</sub>, ranges from 6.73 to 8.95 wt%, and Al<sub>2</sub>O<sub>3</sub> typically ranges from 0.47 to 1.09 wt%. These are within the range of values reported from serpentinized ultramafic samples recovered during DSDP Leg 82. The abundances of other major elements are predictably low: CaO is typically <0.10 wt%, although two samples reach 0.78 wt% (Table 4); MnO ranges from 0.08 to 0.16 wt% in all samples, and the usual ranges for TiO<sub>2</sub>, Na<sub>2</sub>O, K<sub>2</sub>O, and P<sub>2</sub>O<sub>5</sub> are all less than 0.02 wt%. Several samples fall outside the typical ranges of concentrations of major elements and are discussed below; these include Sample 125-778A-2R-1, 89–92 cm, which has low Al<sub>2</sub>O<sub>3</sub> (0.00 wt%) and high CaO (3.52 wt%) and Sample 125-778A-13R-2, 8–11 cm, which has high Al<sub>2</sub>O<sub>3</sub>.

#### Trace Elements

Concentrations of the compatible elements are predictably high (Fig. 3B). In all except two of the samples, values for nickel range from 2173 to 3039 ppm, whereas chromium is more restricted, ranging from 2260 to 2785 ppm. As expected for residual mantle material, the concentrations of incompatible elements (niobium, zirconium, strontium, and rubidium) are low, ranging from not detected (nd) to 2 ppm (2 ppm is below detection limit for niobium, which therefore should be considered present in trace amounts). Each transition element falls within a fairly restricted range: zinc from 28 to 64 ppm; vanadium from 22 to 62 ppm; and copper from 2 to 14 ppm. Cesium and barium are typically below their detection limits. There are no significant correlations between the concentrations of trace elements and depth.

Of the two samples that do not follow the patterns described above, Sample 125-778A-2R-1, 89–92 cm, has a low concentration of chromium (501 ppm), a high concentration of strontium (595 ppm), and falls at the low end of the ranges for vanadium (22 ppm) and zinc (28 ppm) and the high end of the nickel range (3039 ppm). With the notable exception of strontium, this sample is indistinguishable from the other samples on the basis of the more incompatible elements. High concentrations of strontium may indicate the presence of some unusual phase, such as plagioclase, which is not seen in thin section, or it may suggest that strontium is accommodated in secondary minerals, such as carbonates, which are found within the serpentine veins. The low concentrations of chromium may indicate significant alteration of chromite to magnetite or a low proportion of chromite in the sample. Sample 125-778-12R-2, 8–11 cm, has low values of both chromium (837 ppm) and nickel (571 ppm) and slightly high values of strontium (31 ppm) and vanadium (75 ppm). The precise significance of these values is not clear at this stage, although secondary vein materials may be responsible for diluting the abundances of nickel and chromium and enhancing the abundance of strontium.

#### Mafic Rocks

Several types of mafic rocks are present. The majority of samples analyzed are aphyric and contain microphenocrysts of clinopyroxene (15–25 modal %) and plagioclase (10–30 modal %) in an altered glassy matrix (originally 50–90 modal

%). Original glass is now altered, primarily to clays, and samples are heavily veined.

#### Major Elements

Mafic samples also have high LOI, ranging from 1.74 to 7.30 wt% (Table 6), reflecting extensive metamorphism and alteration. Despite the obvious effects of alteration on the more mobile elements, major element compositions suggest that the samples belong to three groups.

Group 1 contains one sample (125-778A-5X-1, 7–10 cm) with 56.03 wt% SiO<sub>2</sub>. This sample also has low iron (Fe<sub>2</sub>O<sub>3</sub> 8.02 wt%) and moderately high MgO (7.57 wt%). Other chemical characteristics include low TiO<sub>2</sub> (0.28 wt%), high total alkalis (5.18 wt%), and especially high Na<sub>2</sub>O (5.03 wt%). This sample may be classified as a high-magnesium andesite (boninite) on the basis of major element criteria, although there is no primary petrographic evidence to support this classification.

Group 2 also consists of only a single sample (125-778A-11X-1, 0–3 cm) and is characterized by high abundances of TiO<sub>2</sub> (2.29 wt%), very high Fe<sub>2</sub>O<sub>3</sub> (18.21 wt%), high P<sub>2</sub>O<sub>5</sub> (0.23 wt%), and high Na<sub>2</sub>O (4.89 wt%). In addition, this sample has low abundances of Al<sub>2</sub>O<sub>3</sub> (6.31 wt%) and MgO (11.73 wt%), and may be classified as a ferrobalt.

The remaining four samples fall into a single group, Group 3. All Group 3 samples are of basaltic composition and are characterized by mid-range values of TiO<sub>2</sub> (0.91–1.12 wt%), lower total alkalis (typically 0.94 to 1.73 wt%) and higher LOI (3.78–7.30 wt%). SiO<sub>2</sub> is variable, ranging from 40.01 to 46.44 wt%. Values of CaO typically range from 9.24 to 12.29 wt%, but are unusually high (17.38 wt%) in one sample (125-778A-13X-1, 5–8 cm), probably a result of carbonate veining. Sample 125-778A-13-CC, 4–6 cm, may also be included in Group 3, but this sample has high abundances of MgO (21.81 wt%), probably reflecting serpentine veining and low CaO (6.09 wt%).

#### Trace Elements

Trace-element compositions are presented in Table 7. The samples making up Group 1 are characterized by lower concentrations of zirconium (31 ppm), yttrium (9 ppm), vanadium (215 ppm), and zinc (56 ppm) than Groups 2 and 3. Group 2 has the highest concentration of zirconium (150 ppm), yttrium (62 ppm), and vanadium (494 ppm) of the three groups, and very high concentrations of nickel (563 ppm). Group 3 has mid-range values of zirconium (50–64 ppm), yttrium (21–28 ppm), and vanadium (242–357 ppm).

The concentration of nickel is almost constant in Group 3 samples and ranges from 41 to 47 ppm. Sample 125-778A-13X-CC, 4–6 cm, exhibits some unusual abundances of trace elements, most notably very low nickel (28 ppm) and chromium (43 ppm), but abundances of vanadium (281 ppm), zirconium (78 ppm), and yttrium (28 ppm) are typical of Group 3.

The three groups, recognized on the basis of major elements, can also be discriminated on the basis of trace elements. Two examples are given in Figure 3: (A) an yttrium/chromium (Y/Cr) diagram after Pearce and Wanming (1988) and (B) a zirconium/titanium (Zr/Ti) diagram after Pearce and Cann (1973). Group 1, the high-magnesium andesite, falls on the boninite-island-arc tholeiite (IAT) boundary of Figure 3A and beyond the lower end of the IAT field in Figure 3B, which overlaps with a boninite field not shown in this diagram. The ferrobalt of Group 2 plots clearly in the mid-ocean ridge basalt (MORB) field of Figure 3A. Although it falls outside the MORB field toward higher titanium and zirconium in Figure

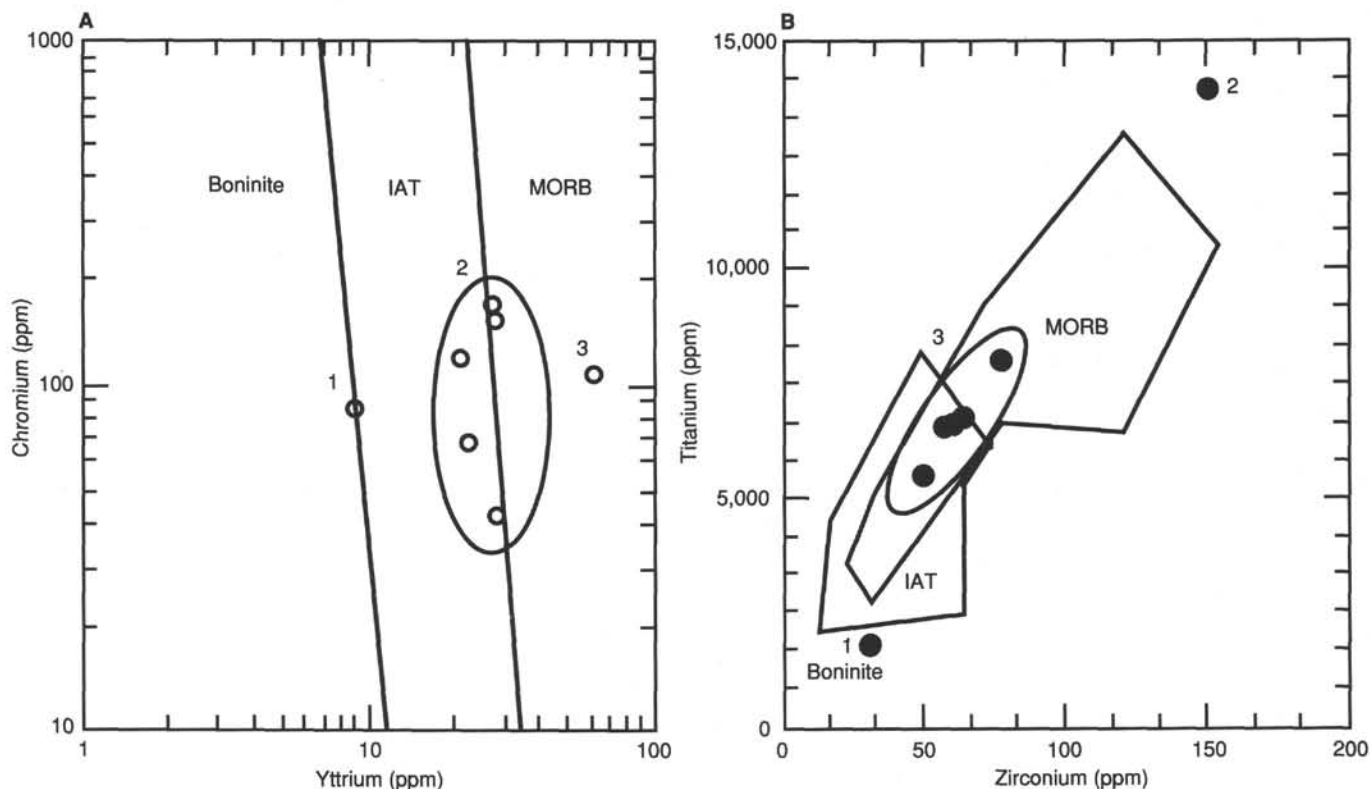


Figure 3. A. Discriminant diagram for tectonic environment of mafic rocks, using log Cr vs. log Y. Samples plotted are mafic clasts from Site 778. Numbers refer to groups defined in the text. Fields are after Pearce and Warming (1988). B. Discriminant diagram for tectonic environment, using Zr and Ti for mafic basaltic rocks. Samples plotted are mafic clasts from Site 778. Numbers refer to groups defined in the text. Fields are from Pearce and Cann (1973).

3B, the composition of the Group 2 sample is comparable to that of ferrobasalts from propagating rifts in oceanic environments. The Group 3 samples form a coherent group in both discrimination diagrams (Figs. 3A and 3B), plotting near the IAT-MORB boundary in both cases. At this stage we cannot be certain whether these samples are IAT, MORB, or transitional between the two.

We stress that these types of diagrams are not perfectly reliable for determining the tectonic provenance of individual or small groups of samples. Although more data are clearly required to make a confident interpretation of tectonic environment, it is apparent that the mafic clasts may have come from at least three different settings, incorporating magma types of both supra-subduction zone and MORB affinities.

## SEDIMENT/FLUID GEOCHEMISTRY

### Sediment Geochemistry

Cores from Site 778 were analyzed on board ship for inorganic carbon and for total carbon, nitrogen, and sulfur, using the techniques described in the "Explanatory Notes" (this volume). The organic carbon content was then calculated by difference. These results are presented in Table 8 and in Figure 4. Except for one near-surface interval, the cores are uniformly carbonate-poor, with concentrations ranging from 0.3 to 4.2 wt%  $\text{CaCO}_3$ . The interval that is relatively carbonate-rich lies between 3 and 6 mbsf and contains 13 to 16 wt%  $\text{CaCO}_3$ . The organic carbon content is also uniformly low, ranging from less than 0.01 to 0.29 wt%. Total sulfur ranges from less than 0.10 to 0.18 wt%, and nitrogen from less than 0.05 to 0.10 wt%. At these low levels, nitrogen may be affected by contamination by air inadvertently included with the sample charge.

### Fluid Geochemistry

The concentration of hydrocarbon gases measured in 5-cm<sup>3</sup> headspace samples is uniformly low (Table 9). Methane was the only gas detected.

Interstitial waters squeezed from the cores have compositions that differ considerably from that of seawater (Table 10). The pH of the waters from Site 778 varies from 8.5 to 9.1 (Fig. 5). This is about 0.5 to 1 pH unit higher than that measured in interstitial waters from normal deep-sea sediments. The high pH presumably results from reaction with the serpentine mineral assemblage. Alkalinity is uniformly low at one-third to one-half the concentration in seawater. Ammonia increases over nearly the entire sampled interval, but never exceeds 90 mmol/kg. Concentrations of dissolved silica are also low, less than 150 mmol/kg, relative to those in more typical deep-sea sediments and even in ocean bottom water in this area, which contains about 150 mmol/kg. The samples from 84 to 100 mbsf have higher silica concentrations than those from the upper 50 m. Where measured within the upper 6 m of sediment, phosphate is also low (Table 10). Sulfate decreases to about one-half the seawater value over the upper 50 m of the section, then apparently rebounds to a constant value of about 17 mmol/kg between at least 84 and 100 mbsf. Magnesium decreases by more than 99% to very low concentrations; most of this change occurs within the upper 50 m of unconsolidated serpentine (Fig. 6). Calcium and sodium each increase by about 15 mmol/kg over the same interval, thereby accounting for less than one-half of the electrical charge loss associated with the removal of magnesium from solution. Potassium remains constant over the upper 50 m, then decreases by a third over the lower 50 m. Most notably, both salinity and chlorinity decrease nearly linearly with depth, by a total of

**Table 8. Total nitrogen, sulfur, and carbon, organic carbon, and carbonate carbon in cores at Site 778.**

Core, section, interval (cm)	Depth (mbsf)	Total nitrogen (wt%)	Total sulfur (wt%)	Total carbon (wt%)	Inorganic carbon (wt%)	Organic carbon (wt%)	CaCO <sub>3</sub> (wt%)
125-778A-							
1R-1, 77-78	0.77				0.51		4.2
1R-1, 117-118	1.17				0.10		0.8
1R-2, 135-136	2.85				1.72		14.3
1R-3, 115-116	4.15	0.075	0.10	1.51	1.63	0.00	13.6
1R-4, 117-119	5.67				1.87		15.6
1R-5, 15-16	6.15				1.92		16.0
2R-1, 15-16	6.85	0.061	0.13	0.51	0.44	0.07	3.7
2R-1, 45-46	7.15				0.51		4.2
5R-1, 14-16	29.84	nd	0.18	0.30	0.11	0.19	0.9
6R-1, 54-56	39.74	0.12	nd	0.35	0.13	0.22	1.1
6R-1, 57-58	39.77	0.096	0.14	0.46	0.27	0.19	2.3
6R-1, 120-121	40.40				0.16		1.3
6R-1, 125-126	40.45				0.25		2.1
7R-1, 67-69	49.37				0.08		0.7
7R-1, 117-118	49.87	0.088	0.098	0.27	0.12	0.15	1.0
7R-2, 36-37	50.56				0.09		0.7
7R-2, 72-73	50.92				0.11		0.9
8R-1, 83-84	59.03				0.13		1.1
8R-1, 137-139	59.57	0.056	0.12	0.17	0.28	0.00	2.3
9R-1, 87-89	69.07	0.079	0.10	0.24	0.11	0.13	0.9
9R-1, 148-149	69.68				0.15		1.2
9R-2, 30-31	70.00				0.23		1.9
11R-1, 20-21	82.50				0.14		1.2
11R-1, 71-73	83.01	0.073	nd	0.68	0.39	0.29	3.3
11R-1, 106-108	83.36				0.13		1.1
11R-1, 133-134	83.63				0.30		2.5
12R-1, 8-9	89.88	0.076	nd	0.50	0.44	0.06	3.7
12R-1, 45-46	90.25				0.22		1.8
12R-1, 75-76	90.55				0.04		0.3
12R-2, 18-19	91.48				0.11		0.9
12R-2, 42-43	91.72	0.068	0.46	0.39	0.15	0.24	1.3
12R-2, 60-61	91.90				0.10		0.8
13R-1, 50-51	98.80				0.21		1.7
13R-1, 81-83	99.11	nd	nd	0.46	0.25	0.21	2.1
13R-1, 115-116	99.45				0.9		0.8

nd = not detected.

almost 10% at 100 mbsf (Fig. 7). The bromide data are highly scattered and show no obvious trend with depth.

### STRUCTURAL STUDIES

The foliated and clastic serpentines recovered at this site are highly disturbed, especially in lithologic Unit II, where the layers are affected by intense plastic deformation (folding) and ductile shearing. This deformation seems to have occurred in the presence of high fluid contents; indeed, the cores shrunk considerably during drying. The tracers of this deformation are convolutions of the layering, asymmetric shapes of poorly consolidated serpentine clasts, development of a foliation, and the presence of shear bands.

#### Convolutions of the Layering

Small-scale layering within Unit II is most often defined by alternating zones of gravelly serpentine sediments and flows of different colors. These layers show abundant convolutions that develop successively as irregular folds, varying from open to tight (Fig. 8). Because of the folding, the attitude of the layering varies from horizontal to vertical (Fig. 9). Often, two or more fold hinges may face in opposite directions, which increases the chaotic appearance of the deformed material. Opposite-facing folds may be concentrated on both sides of the core, so that the central part of the column shows a vertical layering, as seen, for example, in the bottom of Section 125-778A-9R-1 and in Section 125-778A-6R-1, 115-130 cm (Figs. 8 and 10).

Trains of millimeter-sized serpentinite fragments within the unconsolidated serpentine also outline the deformed layering. As in the previous case, this sedimentary layering is a clear tracer of the plastic deformation.

#### Shape of Poorly Consolidated Clasts

Some clasts of strongly altered serpentinite exhibit asymmetric shapes characteristic of a ductile, noncoaxial shearing. We noted, however, that the lithified clasts exhibit no deformation, although the matrix foliation around them is disturbed.

#### Foliation and Cleavage

A clear foliation, either horizontal or oblique, has developed in certain zones, especially around major shear bands that crosscut the cores. The foliation is emphasized both by alignment of stretched millimeter- to centimeter-sized serpentinitic, altered clasts and by discontinuous, sheared laminae. A thin anastomosing cleavage similar to the scaly-clay cleavages (argille scagliose) has also developed, almost parallel to the foliation (Fig. 11). This cleavage is locally emphasized by the development of very pale green laminae (chrysotile-rich laminae?). Further detailed investigations will be required to determine the origin and significance of this cleavage. A preliminary study of the microfabric of the poorly consolidated matrix was conducted using impregnated thin sections. This analysis confirms that the foliation is well defined locally by the preferred orientation of the

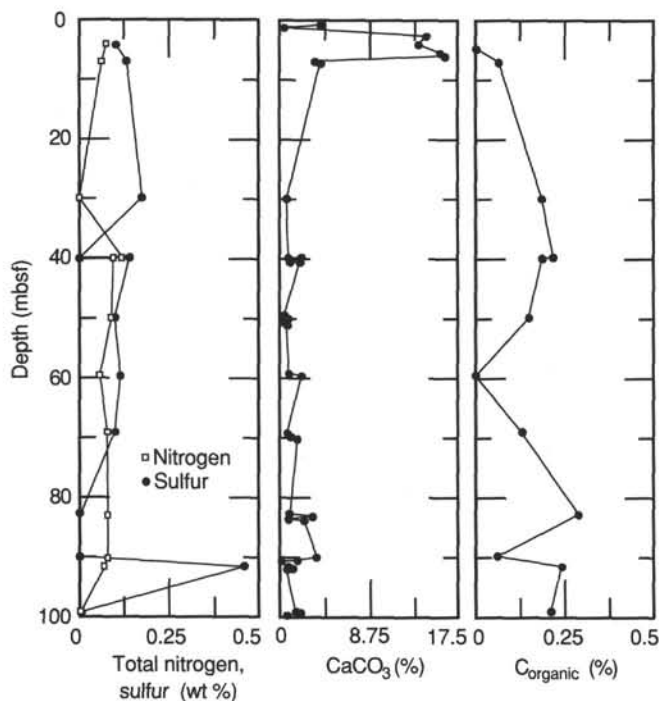


Figure 4. Weight percent of calcium carbonate, total organic carbon, and total nitrogen and sulfur in cores at Site 778.

serpentine flakes. This preferred orientation is visible under crossed nicols, where contiguous portions of the thin sections tend to go to extinction simultaneously. However, on this scale, the deformation is not homogeneous, and a uniform field of deformation cannot be defined. Thus, it would appear that the intensity of deformation has not been sufficient to provide a significant rearrangement of the material.

Hydrogrossular crystals locally form long chainlets and clusters that are located within the foliation planes. Epidote-group minerals (mainly zoisite?) were found within the foliation planes, which indicates that crystallization is pre- to syndeformation. These observations will help constrain models for thermal evolution of the serpentinites.

Decimeter-size folds may affect the foliation, as for example in the bottom of Core 125-778A-9R-1. This observation is confirmed by thin-section analysis that shows tightly folded and sheared serpentine crystals.

Anastomosing foliation planes and curving foliation planes around clasts define shear lenses (phacoids) on all scales (Fig. 12). Lenses may be of millimeter to pluricentimeter scale. In thin section, C-S-type planes also define lenses. However, at this scale, the weakly preferred orientation of the shear planes and lenses does not allow us to define precisely the senses of shear.

### Shear Bands

Shear bands affect the sediments at all scales (mm, cm, dm). Decimeter-sized shear bands can be recognized locally throughout Cores 125-778A-5R to -13R. Oblique bands are particularly visible in Section 125-778A-7R-1 at 85 and 120 cm. Small centimeter-to-millimeter shear bands are abundant within all the sections. These bands deform the foliation defined in the previous section.

Table 9. Results of headspace-gas analyses of cores at Site 778.

Core, section, interval (cm)	Depth (mbsf)	Methane	
		( $\mu\text{L/L}$ ) <sup>a</sup>	( $\mu\text{M}$ ) <sup>b</sup>
125-778A-1R-4, 0-5	4.53	8	1
2R-1, 0-5	6.73	21	2
5R-1, 20-25	29.93	20	2
6R-1, 145-150	40.68	37	3
7R-1, 135-140	50.08	452	40
8R-1, 140-145	59.63	33	3
11R-2, 0-3	83.82	12	1
12R-1, 135-145	91.20	29	3

<sup>a</sup> Microliters of gas per liter of wet unconsolidated serpentine.

<sup>b</sup> Micromoles of methane per liter of interstitial water, assuming a porosity of 50%.

### Discussion

We list here the different mechanisms that may have been responsible for the development of the observed structures:

1. Drilling disturbances;
2. Syn-emplacement slumps, i.e., deformation during pure gravitational flow;
3. Ball-and-pillow structures (density differences in liquefied sediments);
4. Dewatering of very soft sediments (water-escape structures);
5. Fluid-circulation disturbances ("upwelling" of hydrothermal fluids of deep origin); and
6. Purely tectonic processes within the diapir.

Some of these mechanisms may have acted together. A first approach might be to separate the mechanisms responsible for the creation of foliation from those responsible for its subsequent folding. However, during progressive deformation processes, different structures may appear at different successive stages of the evolution so that earlier structures are deformed by the later ones. In that case, the presence of a folded foliation does not mean that two different successive events took place. Further analyses and discussions will be necessary to propose more detailed hypotheses. However, preliminary microstructural analyses conducted on board the ship allow us to propose that the foliation observed within the serpentine sediments and flows of Site 778 is not related to drilling disturbance; the major argument is that the alignment of syntectonic hydrogarnets parallels this foliation.

Finally, the fabric and microfabric displayed by the soft material drilled at Site 778, and more particularly the fact that the layering attitude is often vertical, might suggest the involvement of tectonic processes with vertical component linked to diapiric processes. However, such features may also be interpreted as the result of gravitational flows involving a thick pile of unconsolidated, fluidized, serpentinous debris covering the diapir flanks. The hydrothermal paragenesis also suggests that water circulation is responsible for a significant amount of the nonpenetrative deformation. The presence of horizontal to gently dipping shear zones indicates that horizontal displacement took place on the flank of the diapir. Such displacements can be related to gravitational instability of the upper part of the diapir.

**Table 10. Composition of interstitial waters from Hole 778A cores.**

Sample number	Core, section, interval (cm)	Volume (mL)	Squeeze temperature (°C)	Depth (mbsf)	pH	Salinity (R.I., %)	Salinity (calcium, %)	Chlorinity (mmol/kg)	Alkalinity (meq/kg)	Sulfate (mmol/kg)	Na (mmol/kg)	K (mmol/kg)
Surface seawater (22 February 1989)					8.34	35.4	34.73	539.0	2.410	28.60	461.9	10.12
IW-1	1R-1,145-150	31	2	1.48	9.00	34.5	34.44	542.6	0.985	24.46	475.5	10.22
IW-2	1R-4,145-150	63	2	5.98	8.48	35.5	34.93	547.5	1.185	27.17	469.8	10.21
IW-3	7R-1,140-150	12	4	50.15	8.99	32.3	32.75	532.0	0.827	12.15	488.7	10.09
IW-4	11R-1,140-150	15	3	83.75	8.94	30.8	32.33	510.7	1.339	16.83	486.4	8.60
IW-5	12R-1,140-150	10	5	91.25	9.14	30.0	31.78	502.0	1.339	16.43	477.1	8.47
IW-6	13R-1,140-150	12	6	99.75	8.86	31.2	32.07	508.8	0.783	16.77	484.9	6.71

Note: Values absent from table were not determined.

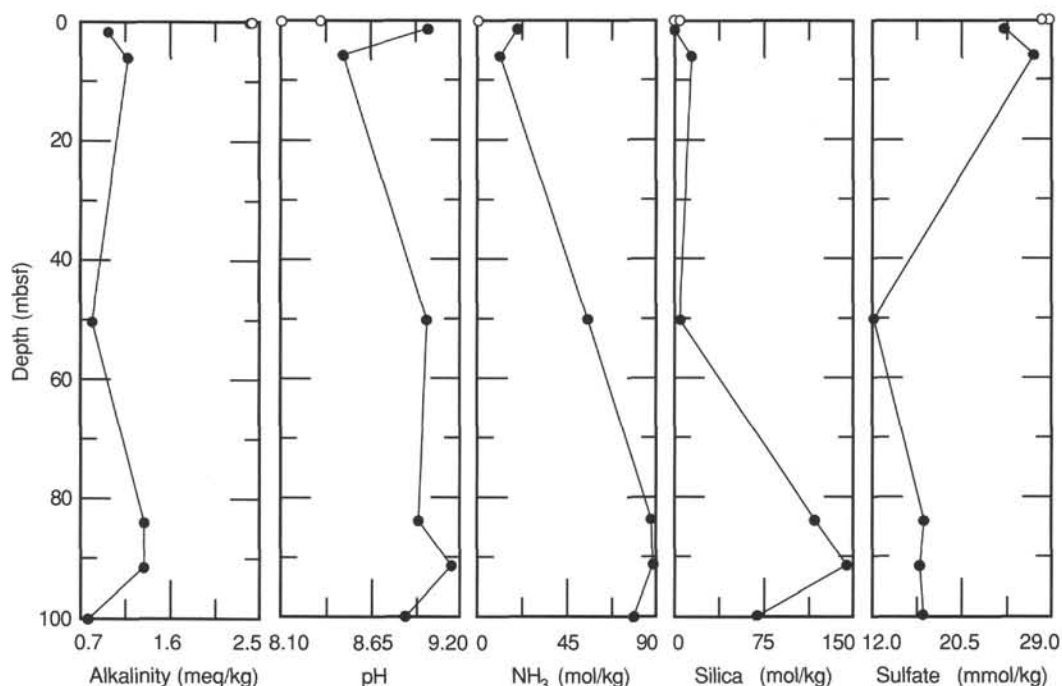


Figure 5. Composition of interstitial waters from cores at Site 778 (closed circles), compared with surface seawater collected 22 February and 4 March 1989 (open circles).

## PALEOMAGNETISM

Owing to the extremely poor recovery, the tectonized nature of the rocks, and the limited number of stratigraphic units at Site 778, magnetostratigraphy was nearly impossible. The natural remanent magnetization (NRM) of the archive half of each core was measured using the cryogenic magnetometer. Core 125-778A-2R and Cores 125-778A-4R through 125-778A-11R were demagnetized with the on-line alternating-field (AF) demagnetizer and measured at the 5 and 10 mT levels. Cores 125-778A-1R, -12R, and -13R were demagnetized and measured at the 3, 5, 8, and 10 mT levels.

The only useful magnetostratigraphic information from Site 778 is from Interval 125-778A-1R-1, 50 to 150 cm (0.5–1.5 mbsf). A reversed component of magnetization is evident in this interval (Fig. 13). The top of the serpentine flow must therefore be at least as old as the last reversal at 0.73 Ma (Berggren et al., 1985, and biostratigraphic evidence in "Biostratigraphy" section, this chapter), and very little deposition must have occurred since the time when the flow was deposited.

Within the serpentinite material (lithologic Unit II), some of the more coherent pieces of core exhibited a consistent

magnetization. Negative inclinations were measured in Intervals 125-778A-5R-1, 0 to 43 cm (29.7–30.1 mbsf), 125-778A-12R-1, 0 to 150 cm, and 125-778A-12R-2, 0 to 90 cm (89.8–92.2 mbsf). Positive inclinations were measured in the Intervals 125-778A-7R-1, 0 to 140 cm (48.7–50.1 mbsf), and 125-778A-11R-1, 10 to 140 cm (82.4–83.7 mbsf). However, because of the lack of stratigraphic and age control, and the extremely metamorphosed and deformed state of the rocks, it is impossible to place these data into a tectonic or geochronological framework.

The intensities throughout the section were high, ranging from approximately 10 to 100 mA/m. This is not surprising considering that magnetite is a common secondary product of the serpentinization process.

Magnetic susceptibilities were measured with a Bartington Instrument susceptibility meter on the multisensor track, the first time this configuration of the system was tried. However, problems with the program and the instrument prevented acquisition of meaningful data.

## PHYSICAL PROPERTIES

Physical properties for Site 778 were measured on both whole-round and discrete samples (Table 11). The multisensor

Table 10 (continued).

Ca (mmol/kg)	Mg (mmol/kg)	Br (mmol/kg)	Si ( $\mu$ mol/kg)	NH <sub>3</sub> ( $\mu$ mol/kg)	PO <sub>4</sub> ( $\mu$ mol/kg)
10.40	52.89	0.83	<5	<5	
10.25	43.16	1.00	<5	20	0.27
8.90	52.59	0.95	15	11	0.16
20.76	8.41	1.07	5	55	
23.90	1.43	0.87	117	87	
24.79	0.55	1.19	143	87	
21.03	4.70	0.97	68	78	

track (MST) and thermal conductivity measurements were performed on whole-round samples, and representative discrete samples were taken from working halves of split cores (Table 12). The compressional-wave velocity logger on the MST did not couple well with the incompletely filled liners, and thus no data were recorded. The gamma-ray attenuation porosity evaluator (GRAPE) was used on all sections. Considerable scatter is apparent in the data, related to incompletely filled liners that introduced artificially large porosity values. Magnetic susceptibility was also measured on the MST; however, the instrument was malfunctioning, and only erratic readings were recorded.

Thermal conductivities from the serpentinites were measured with needle probes, giving values ranging from 0.96 to 2.72 W/mK. The higher values of conductivity are associated with the more water-rich (slurrylike) serpentine sediments and flows.

Measurements of compressional-wave velocity and index properties (wet and dry volumes, wet and dry masses, porosity, and water content) were performed, and values calculated for discrete samples. Hamilton frame velocity measurements were not performed for soft serpentine samples, as these were too mobile to be placed in the apparatus. More compact serpentinites were measured, giving velocities ranging from 2.1 to 4 km/s. Bulk densities and water content, derived from

the index properties, were highly variable and dependent upon the water contained in the sections. Porosities were generally in excess of 40%, with values as high as 86%, and water content closely followed these trends. The index properties from Site 778 probably reflect the water entrained in the cores by drilling, rather than the *in-situ* values.

## SUMMARY AND CONCLUSIONS

Site 778 (19°29.93'N, 146°39.94'E; water depth, 3913.7 m) is situated about halfway up the southern flank of Conical Seamount, a 1500-m high cone-shaped serpentine seamount located on the outer-arc high of the Mariana forearc basin, about 100 km west of the trench axis. Site selection was based on a SeaMARC II side-scanning sonar image of the seamount, which indicated recent serpentine flows as areas of high sonar backscatter. The site is located in the center of a major flow.

Hole 778A was spudded at 1445UTC on 22 February 1989 and was RCB-cored to 107.6 mbsf. Episodes of instability of the hole required that the hole be repeatedly washed out, and finally, at 0700UTC on 24 February, prevented further drilling. This lack of stability was attributed to the friable and heterogeneous nature of the serpentine flows (hard clasts of variable size in a soft matrix). Recovery of the cored intervals was low, averaging 21% overall and only 13.7% in Unit II (Fig. 14).

Two lithologic units can be recognized at Site 778: a serpentine-rich clay-marl-breccia (Unit I) and a phacoidal sheared serpentine (Unit II).

Unit I (Subunit IA, 0–7.2 mbsf): The subunit consists of lower/middle Pleistocene-Holocene(?) serpentine-rich sediment and serpentine flows. The uppermost portion has two pebbles (one limestone and one serpentine) overlying 15 cm of pale blue-gray serpentine clay. Below this is 15 cm of gray-green serpentine clay, 10 cm of red-orange serpentine clay, and 1.5 m of pale blue-gray, silt-sized serpentine (containing 80% serpentine, 10% opaque minerals, 10% epidote-group minerals, and trace amounts of chlorite, glass, and

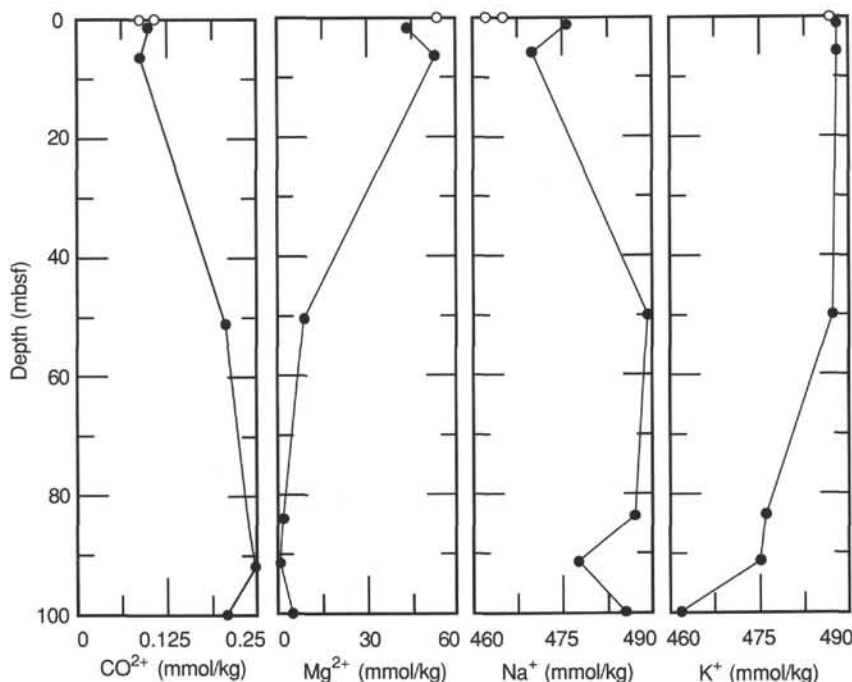


Figure 6. Composition of interstitial waters from cores at Site 778 (closed circles), compared with surface seawater collected 22 February and 4 March 1989 (open circles).

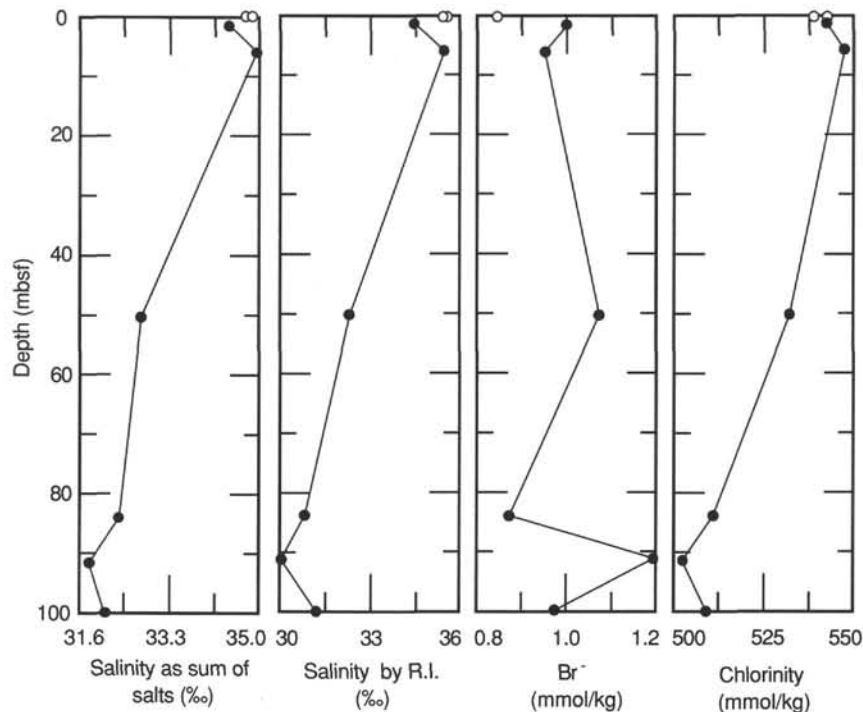


Figure 7. Composition of interstitial waters from cores at Site 778 (closed circles), compared with surface seawater collected 22 February and 4 March 1989 (open circles).

micrite). The bottom of this unit is a breccia that extends to the base of Core 125-778A-1R (an interval of 357 cm) and through the upper 50 cm of Core 125-778A-2R. The upper 0.9 m of the breccia is composed of serpentine and exhibits extensive drilling disturbance; the remainder has a light reddish-brown matrix of sandy- to silt-sized serpentine, occasionally mottled by mixing with a light-gray and light-olive serpentine-chlorite rich marl. The admixture of detrital and serpentine material within this subunit may indicate either drilling disturbance or incorporation of sediment in a remobilized serpentine flow.

Unit I (Subunit IB 7.2–29.8 mbsf): This subunit is lower-middle Pleistocene to lower Pleistocene(?) and contains sandy marl and a collection of cobbles and pebbles, including serpentinite, vesicular volcanic rocks, and a foraminifer-bearing serpentine sandstone.

Unit II (29.8–107.6 mbsf): This entire unit is made up of phacoidal, sheared serpentine. Its matrix is composed of serpentine (50%–80%), opaque minerals (20%–5%), epidote-group minerals, some manganese-rich (thulite) (25%–0%), chlorite (15%–0%), talc (5%–0%), olivine (5%–0%), and albite and micrite (trace–0%). A variety of clasts are present: variably serpentinized tectonized harzburgite (80%); metabasalts (15%); and a variety of other fragments, including metagabbros, serpentinized dunites, and vein materials such as talc, carbonates, and quartz (5%).

The 1.5 m of silt-sized serpentine in Subunit IA has been interpreted as a serpentine flow, rather than a pelagic sediment because of the lack of pelagic or detrital components, the atypical color, and the absence of biological or sedimentological structures. The mottled interval below this layer may also be a flow, but contains both detrital and serpentine materials.

Dating has been based on the magnetostratigraphy and sparse biological components. In the interval from 0.5 to 1.5 mbsf, a reversed component of magnetization gives a minimum age of 0.73 Ma, the age of the last reversal. Biostratigraphic data

indicate an early/middle Pleistocene age in Subunit IA at 7 mbsf and an early Pleistocene age in Subunit IB (approximately 1.7 Ma) at 29.5 mbsf. The youngest serpentine flows can thus be dated as Pleistocene. There has been little sediment accumulation since the youngest flow was deposited.

The ultramafic clasts in the cores are of two types: serpentinized, tectonized harzburgite (70%–90% serpentine and estimated protolith composition of 70%–85% olivine, 25%–15% orthopyroxene, with minor quantities of clinopyroxene [mainly as exsolution lamellae in orthopyroxene] and a chromium-rich spinel) and serpentinized dunite. There are several types of variably metamorphosed mafic clasts in the cores. These include metamorphosed volcanics that contain plagioclase-clinopyroxene and/or orthopyroxene phenocrysts or orthopyroxene-olivine-chromium spinel phenocrysts in a glassy groundmass. One metagabbro was observed. A few metabasalts show medium-grade metamorphism (one sample contains blue amphibole rimming green amphibole).

The serpentine flow sequence in lithologic Unit II exhibits a number of structural features, including deformation of primary orthopyroxene, microbrecciation, ductile shearing of clasts, shear zones on all scales (mm, cm and dm) and orientations, a variably developed foliation parallel to shear-plane orientations, and open-to-isoclinal folding of bedding and foliation planes. These features can be interpreted in terms of a combination of primary mantle tectonism, stresses related to intrusion and protrusion (flow emplacement) of the serpentinite diapir materials, and stresses resulting from post-protrusion remobilization.

Analyses of interstitial pore-water samples show a 10% decrease in chlorinity downhole (over 107 m). This observation is consistent with the low (relative to seawater) chlorine content of fluids seeping from chimneys at the summit of the seamount (collected with *Alvin*). These seep fluids are thought to have formed in part as a product of dehydration reactions within the subducting Pacific Plate. The decrease in chlorinity with depth in the hole is inter-

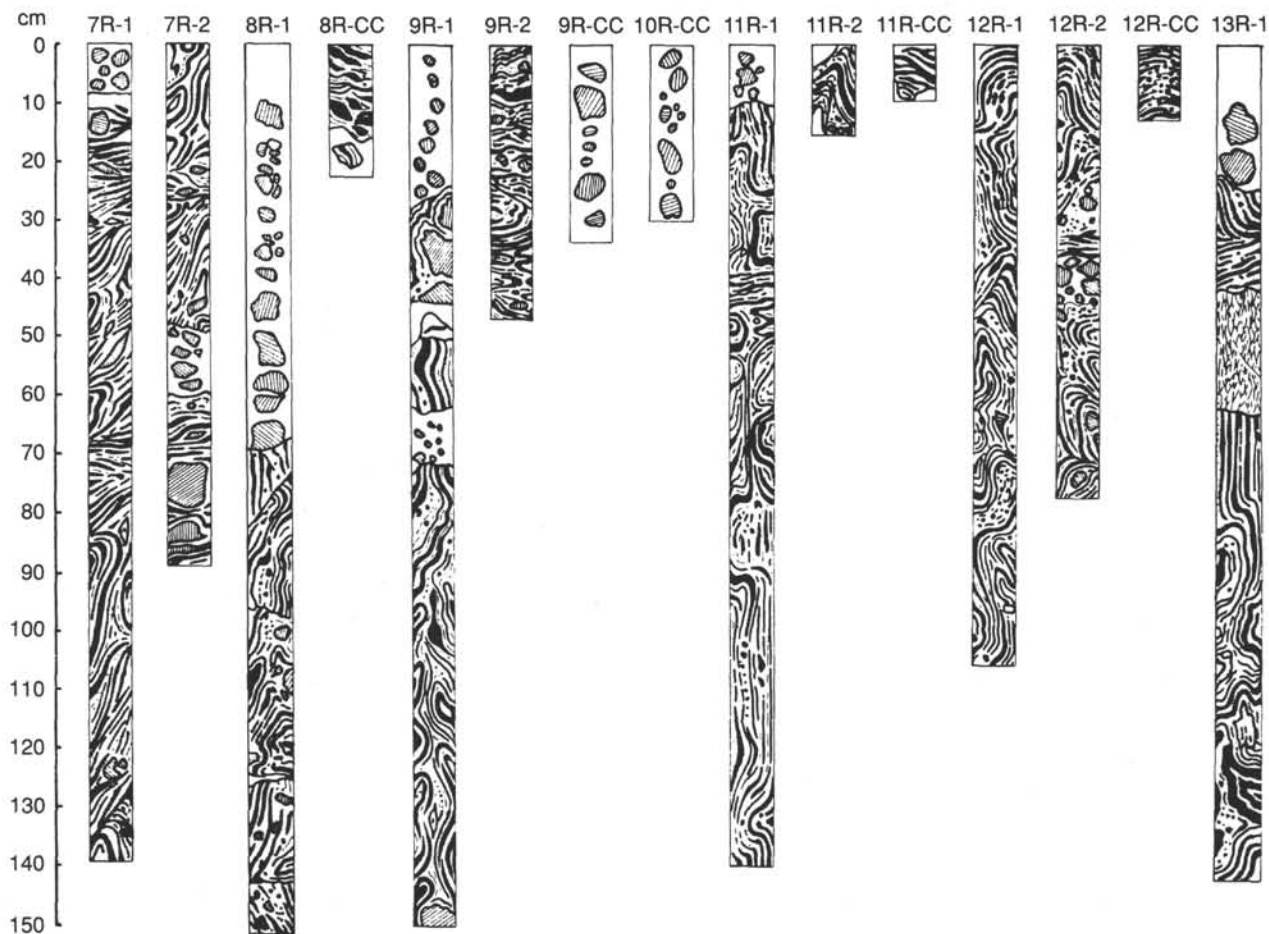


Figure 8. Structural features of Cores 125-778A-7R to 125-778A-13R showing the main outlines of the plastic deformation affecting the layered serpentine microbreccias.

preted as a relative decrease in admixture of seawater with similarly chlorine-poor fluids entrained in the serpentine flow material (a compaction effect?).

The principal results can be summarized as follows:

1. The confirmation that forearc seamounts can be constructed at least in part from serpentine flows emanating from a central diapir;
2. The evidence from clasts that low- to medium-grade metamorphism characterizes the source region of the serpentinite diapirs; and
3. The evidence from water chemistry that dehydration of the subducted lithosphere may have played an important role in the serpentinization of the source region of the serpentinite diapirs.

#### REFERENCES

- Berggren, W. A., Kent, D. V., Flynn, J. J., and Van Couvering, J., 1985. Cenozoic geochronology. *Geol. Soc. Am. Bull.*, 96:1407-1418.
- Fryer, P., Ambos, E. L., and Hussong, D. M., 1985. Origin and emplacement of Mariana forearc seamounts. *Geology*, 13:774-777.
- Hussong, D. M., and Fryer, P., 1985. Forearc tectonics in the northern Marianas arc. In Nasu, N., Kobayashi, K., Uyeda, S., Kushiro, I., and Kagami, H. (Eds.), *Formation of Active Ocean Margins*: Tokyo (Terrapub), Adv. Earth Planet. Sci., 273-290.
- Kennett, J. P., and Srinivasan, M. S., 1983. *Neogene Planktonic Foraminifera: A Phylogenetic Atlas*: Stroudsburg, PA (Hutchinson Ross).
- Michael, P. J., and Bonatti, E., 1985. Petrology of ultramafic rocks from Sites 556, 558, and 560 in the North Atlantic. In Bougault, H., Cande, S. C., et al, *Init. Repts. DSDP, 82*: Washington, (U.S. Govt. Printing Office), 523-528.
- Okada, H., and Bukry, D., 1980. Supplementary modification and introduction of code numbers to the low-latitude coccolith biostratigraphic zonation (Bukry, 1973; 1975). *Mar. Micropaleontol.*, 5:321-325.
- Pearce, J. A., and Cann, J. R., 1973. Tectonic setting of basic volcanic rocks determined using trace element analysis. *Earth Planet. Sci. Lett.*, 19:290-300.
- Pearce, J. A., and Wanming, D., 1988. The ophiolites of the Tibetan Geotraverse, Lhasa to Golmud (1985) and Lhasa to Kathmandu (1986). *Phil. Trans. R. Soc. London*, A327:215-238.

Ms 125A-106

**NOTE: All core description forms ("barrel sheets") and core photographs have been printed on coated paper and bound as Section 4, near the back of the book, beginning on page —.**

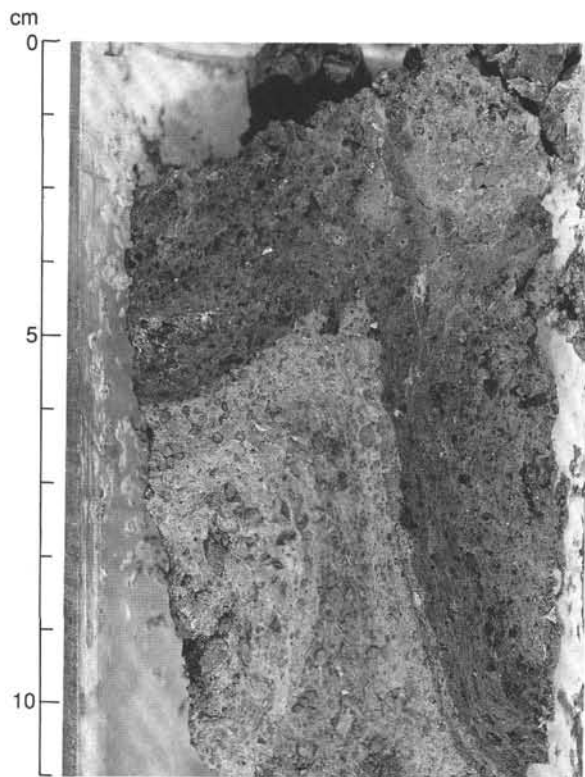


Figure 9. Sample 125-778A-11R-2, 1–11 cm. Fold affecting a layered serpentine microbreccia. Layering varies from horizontal to vertical.

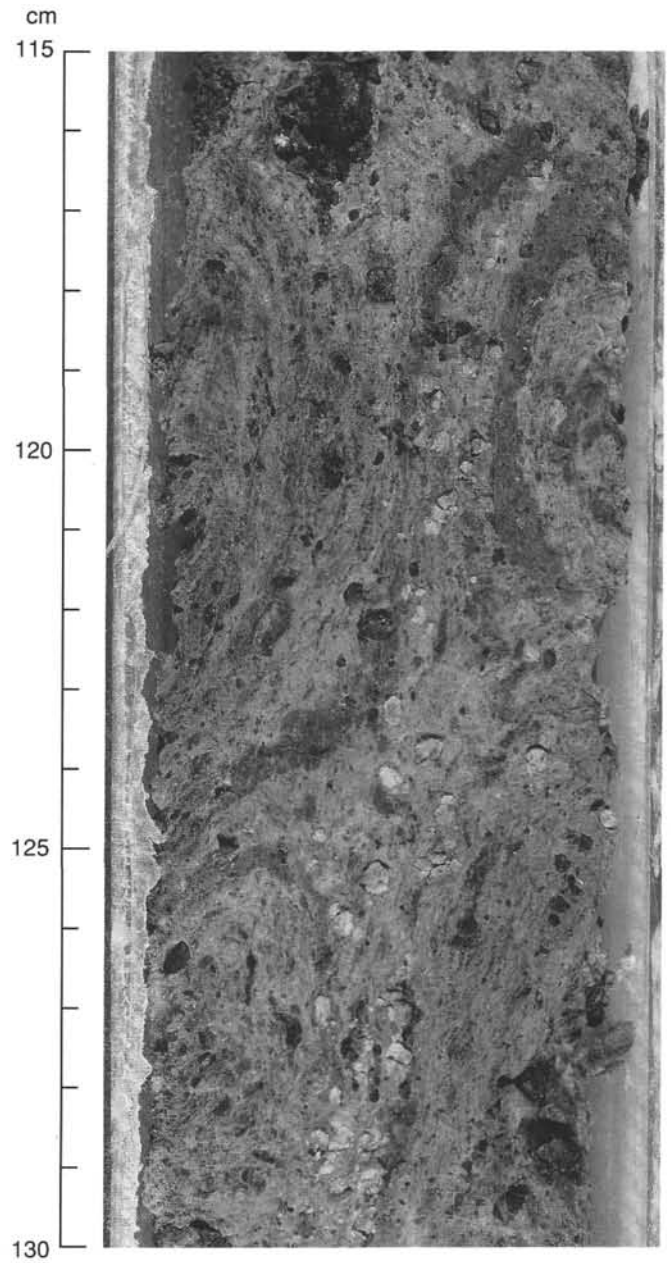


Figure 10. Sample 125-778A-6R-1, 115–130 cm. Folds affecting a layered serpentine microbreccia. In the split plane, the fold hinges are opposite, and the foliation in the central part of the core is vertical. These structures may be drilling disturbances.

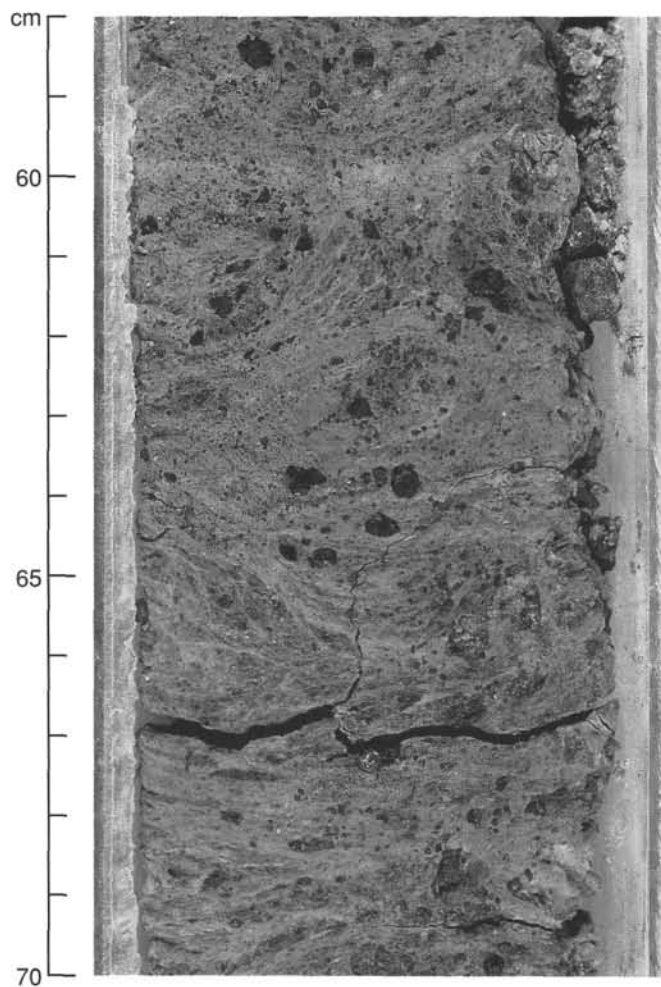


Figure 11. Sample 125-778A-6R-1, 58–70 cm. Foliated layered serpentine microbreccia. Anastomosing cleavage, almost horizontal, defines lenses of different scales. Foliation planes are curved around the coarsest clasts. Poorly consolidated clasts present typical asymmetrical shapes.

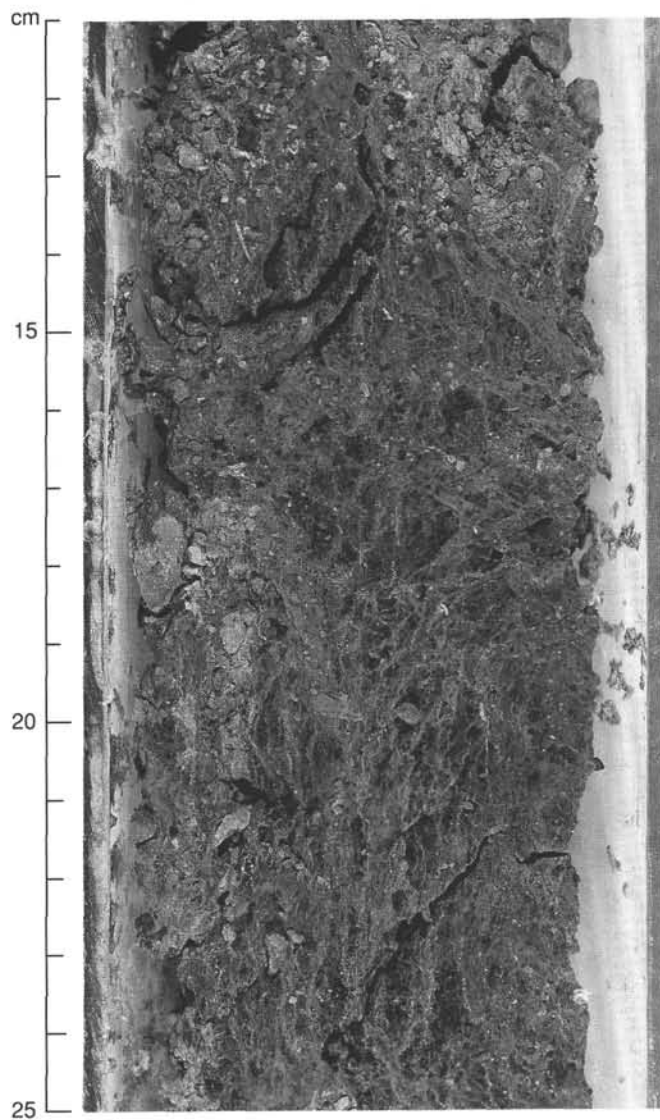


Figure 12. Sample 125-778A-11R-1, 11–25 cm. Sheared phacoidal serpentine. The phacoids are outlined by anastomosing cleavages. The general foliation is vertical.

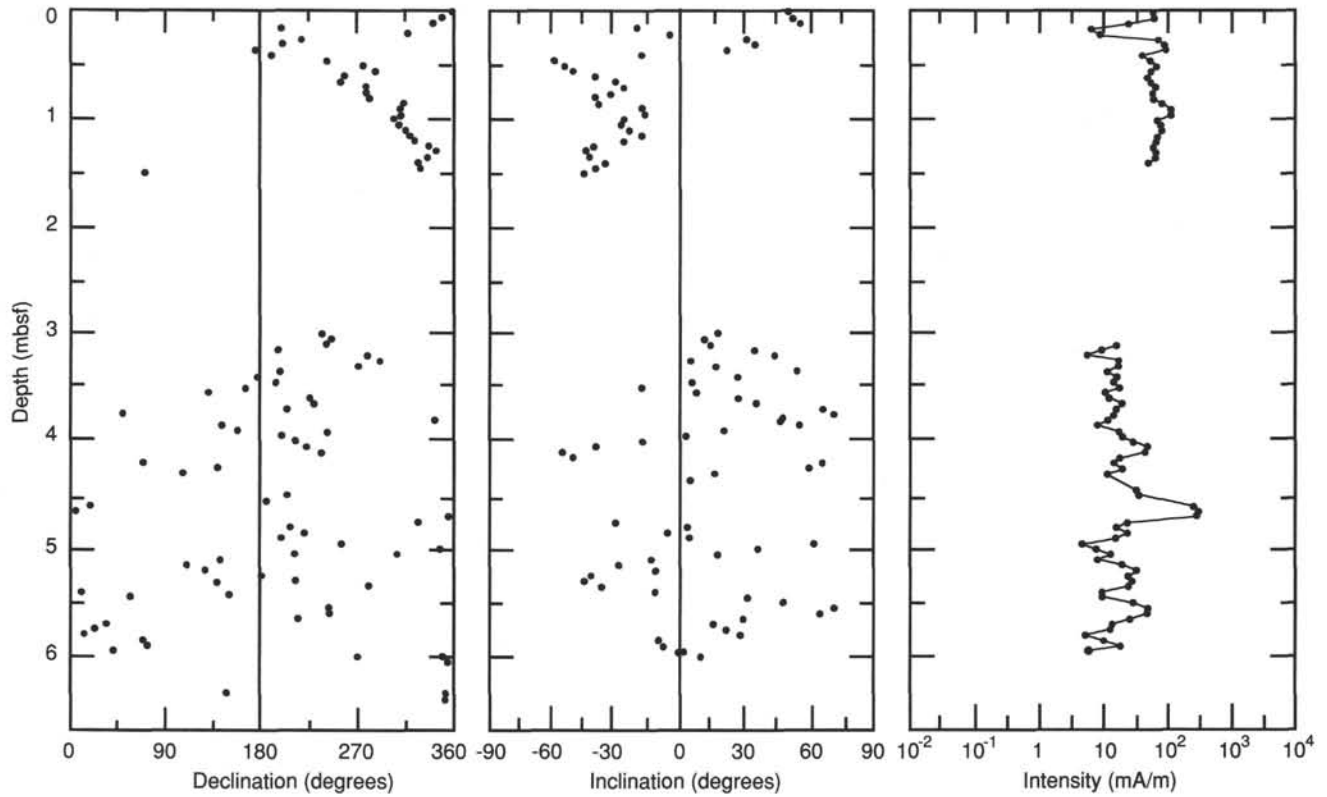


Figure 13. NRM measurement of Core 125-778A-1R. Interval 125-778A-1R-1, 50 to 150 cm (0.5–1.5 mbsf) exhibits a consistently negative inclination, indicating a reversed polarity.

Table 11. Index properties for Hole 778A.

Core, section, interval (cm)	Depth (mbsf)	Bulk density (g/cm <sup>3</sup> )	Grain density (g/cm <sup>3</sup> )	Porosity (%)	Water content (%)	Void ratio
125-778A-						
1R-4, 117–119	5.67	1.53	2.53	67.0	46.5	0.67
5R-1, 14–16	29.84	2.11	2.6	31.3	15.8	0.31
6R-1, 57–58	39.77	1.81	2.84	56.9	33.3	0.57
7R-1, 67–69	49.37	2.39	3.14	35.6	15.8	0.36
8R-1, 83–84	59.03	2.48	3.13	30.9	13.2	0.31
9R-2, 87–89	70.00	2.07	2.84	43.0	22.1	0.43
11R-1, 71–73	83.01	2.14	2.77	36.6	18.1	0.37
11R-1, 106–108	83.36	2.44	3.07	30.6	13.3	0.31
12R-1, 76–78	90.56	2.47	2.99	26.3	11.3	0.26
13R-1, 81–83	99.11	2.70	3.91	42.1	16.5	0.42

Table 12. Physical properties for Hole 778A.

Core, section, interval (cm)	Depth (mbsf)	Thermal conductivity (W/mK)
125-778A-		
1R-1, 50	0.5	1.518
1R-3, 50	3.5	1.219
1R-5, 50	6.5	1.398
8R-1, 132	59.5	1.560
9R-1, 134	69.5	2.725
11R-1, 60	82.9	2.037
13R-1, 73	99.0	1.532

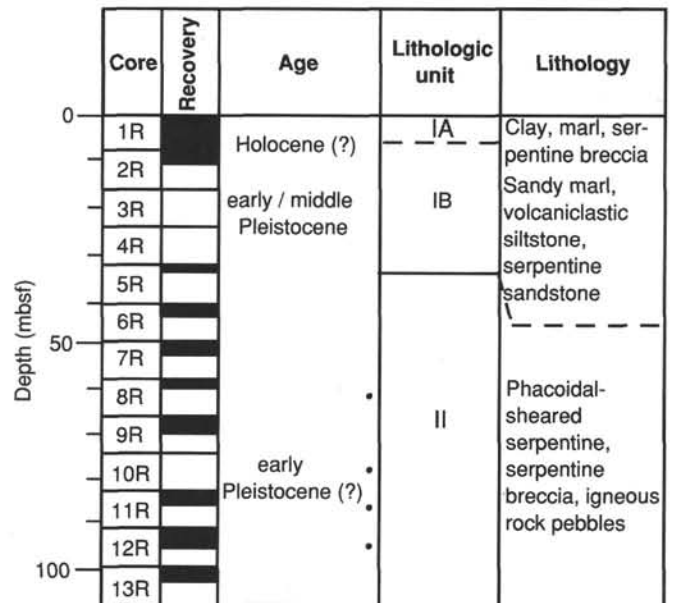


Figure 14. Core recovery and lithologic summary, Hole 778A.